UCSF
UC San Francisco Electronic Theses and Dissertations

Title
Pancreatic Innervation in Mouse Development and Beta Cell Regeneration

Permalink
https://escholarship.org/uc/item/4rc1h6g4

Author
Burris, Regina Elaine

Publication Date
2007-09-06

Peer reviewed|Thesis/dissertation

eScholarship.org Powered by the California Digital Library
University of California

Pancreatic Innervation in Mouse Development and Beta Cell Regeneration

by

Regina E. Burris

DISSERTATION

Submitted in partial satisfaction of the requirements for the degree of

DOCTOR OF PHILOSOPHY

in

Cell Biology

in the

GRADUATE DIVISION

of the

UNIVERSITY OF CALIFORNIA, SAN FRANCISCO

Dedication and Acknowledgements

I dedicate this work to my grandmothers, Hazel S. Burris and Shirley Colvin; to my great aunt Mary Harrison: she never fails to remind me, whenever I turn up, that if she'd known I was coming she'd have baked a cake; to my parents, Barbara E. Morrison neé Colvin, and Stanley H. Burris, who played an immeasurable role in making me who I am (and the older I get, the happier I am about that).

There are so many people without whose support I never would have gotten to this point. First, I would like to thank my research advisor, Matthias Hebrok, and Ulrike Heberlein and Graeme Davis for sitting on my thesis committee and for their support throughout my graduate education. Robert Edwards was an immense help with manuscript preparation, providing much-needed feedback at a critical time. Alo Basu and Katya Delak are two of my closest friends, without whom I would be steady as soup, and they have enriched my life in so many ways that words cannot do them justice. Holly Field is both a domestic and a professional angel, and I thank her for all of the critical support she has provided on all fronts through the years.

My erstwhile classmates Monica Schwartz, Ellie Heckscher, Jennifer Ramond Berman, Joyce Tung, Susanna Mlynarczyk-Evans, Meg Byrne, Dmitri Nusinow, Brian Kelch, and Adam Douglass have all been there for me at different times and in different ways, and I cherish their friendships greatly. Celeste Winant and Rebecca Leonardson have been unflagging and selfless friends since way back. Marcel Bruchez and Robert Moy have given me loads of practical career advice. Ramteen Sioshansi kept me from moping, and generally did a lot to make my last year of graduate school much better than it could have been; I hope I did the same for him. Adrianne Ambrose was an oasis of

sanity for 18 increasingly insane months, and I want to be able to channel her at the required times when I grow up.

My deepening aikido practice has become indispensable, and I never would have made it through graduate school without the harmony it has brought to my life. So I would also like to thank my teachers Penny Sablove Sensei and Linda Holiday Sensei, and just a few of the training partners from whom I have learned so much: Signe Burns, Mark Cohen, Johan Dowdy, Patty Fong, Antonio Long, Geoff Nix, Andrew Penn, and Jessica Ratcliff Kumar.

I want to thank Marina Pasca di Magliano for her comradeship and friendship in lab and in life; Patrick Heiser for all the time he spent answering questions and helping me to hone my microscopy skills; Janet Lau for her practicality and generosity; Sapna Puri for her unfailing ability to get me to look on the bright side; Sara Cervantes for her good cheer; Pedro Gonzales for his listening ear; and Grace Wei, Geraldine Bienvenue, David Cano, John Morris and the rest of the Hebrok lab for making the lab a great place to be.

Ranu-Mashi and Anupam-Kaku Basu were my first (and are my perennial) home away from home, and I'm so happy and proud to be one of their half-a-daughters. Dan Cox taught me a lot about having the right attitude, and had the guts to get angry on my behalf when I lacked the confidence to stand up for myself. Fabrice Roegiers taught me almost everything I know about confocal microscopy. Ming Chan is an über-smart guy who I can't thank enough for giving me the right advice, even before I knew to accept it. Mike Rothenberg also gave me unflinchingly practical advice when I was in dire need,

and made me feel like I could take it without losing face. You were absolutely right, Mike, and I'm so relieved that I had the sense to listen.

Finally, I want to take a moment to thank Dr. Nancy Hopkins, who was my first real scientific mentor; she has been an amazing source of support and inspiration, and I have been so very lucky to learn from her. Dr. Hopkins, thank you.

During the lion's share of this project I was supported by a Ruth L. Kirschstein Predoctoral National Research Service Award from the NIH/NIDDK, and by NIH/NIGMS training grant #1 R25 GM56847. Grants from the NIH (R01 DK60533) and the Juvenile Diabetes Research Foundation (JDRF) have also supported work in Matthias Hebrok's laboratory.

Abstract

Pancreatic innervation is being viewed with increasing interest with respect to pancreatic disease. At the same time, relatively little is currently known about innervation dynamics during development and disease. The present study employs confocal microscopy to analyze the growth and development of sympathetic and sensory neurons and astroglia during pancreatic organogenesis and maturation. Our research reveals that islet innervation is closely linked to the process of islet maturation—neural cell bodies undergo intrapancreatic migration/shuffling in tandem with endocrine cells, and close neuro-endocrine contacts are established quite early in pancreatic development. In addition, we have assayed the effects of large-scale β-cell loss and repopulation on the maintenance of islet innervation with respect to particular neuron types. We demonstrate that depletion of the β-cell population in the RIP-cmyc^{ER} mouse line has cell-type-specific effects on postganglionic sympathetic neurons and pancreatic astroglia. This study contributes to a greater understanding of how cooperating physiological systems develop together and coordinate their functions, and also helps to elucidate how permutation of one organ system through stress or disease can specifically affect parallel systems in an organism.

Table of Contents **Page**

Abstract vi

Chapter 1: Introduction and Background……...1

Introduction 1

Pancreatic Morphology and Organogenesis 4

Neural Crest Development: Neurulation and Migration 5

Chapter 2: Methods……10

Experimental Animals 10

Tissue Preparation and Immunofluorescent Processing 10

RIP-cmyc^{ER} Activation Protocol 12

Immunofluorescent Confocal Microscopy 13

Attempted Direct Fluorescent Labeling of Primary Antibodies 13

Vibratome Section Preparation 14

Chapter 3: Results……...15

Innervation Morphology of the Adult Pancreatic Islet 15

Sympathetic and Sensory Neurons Enter the Pancreatic Bud During Late Embryogenesis (e10.5-18.5) 18

Islet Innervation and Encapsulation Take Place Coincident with Postnatal Islet Maturation (p0-21) 21

Selective Loss of β-cells Differentially Affects Maintenance of Islet Innervation in RIP-cmyc^{ER} Mice 26

Chapter 4: Discussion and Conclusions……32

Innervation and encapsulation of islets occur in tandem with islet maturation 32

The presence of VMAT2 provides clues to the status of autonomic function in developmental and disease states of the pancreas 34

Sympathetic neurons, sensory neurons, and astroglia are differentially affected by large-scale fluctuations in the β–cell population 35

References……40

Appendix 1: Representative Controls……50

Appendix 2: Unpublished Results and Their Implications……..51

Sympathetic nerve development appears unperturbed in Pax4-Shh transgenic mice 51

Partial analysis of parasympathetic pancreatic neurons 52

GRP is not a marker of parasympathetic nerve growth and islet innervation during embryogenesis (e9.5-e18.5) 53

Loss of β-cells in RIP-cmyc^{ER} mice appears to have an intermediate effect on parasympathetic islet innervation 53

A preliminary comparative analysis of autonomic innervation in the non-obese diabetic (NOD) mouse 58

List of Tables **Page**

Table 1: Antibodies Used in Published Analysis 48

Table 2: Additional Antibodies Assayed (not used in published analysis) 49

List of Figures **Page**

Figure 1: The stages of pancreatic organogenesis and maturation 7

Figure 2: Development of the neural crest begins with the process of neurulation 8

Figure 3: Migration of the trunk neural crest occurs in three temporally and positionally distinct waves 9

Figure 4: Pancreatic neurons and astroglia are intimately associated with the islets of Langerhans 16

Figure 5: Adult pancreatic neural processes have distinct modes of perivascular association 17

Figure 6: Sympathetic and sensory cell bodies enter the pancreatic bud during organogenesis 20

Figure 7: Nerve growth and islet innervation during postnatal pancreatic maturation, p0-p15 24

Figure 8: Growth of the sympathetic perivascular plexus during postnatal pancreas maturation 25

Figure 9: Induction of hyperglycemia is followed by recovery of normoglycemia in RIP-cmyc^{ER} mice 29

Figure 10: Differential effects of β-cell loss on sympathetic and sensory neurons and astroglia 30

Figure 11: The structure of sympathetic fibers is intact throughout β-cell loss and resurgence 31

Figure 12: Positive control stainings for the antibodies featured in this analysis 50

Figure 13: Negative control stainings for the antibodies featured in this analysis 50

Figure 14: Pancreatic parasympathetic innervation has similarities with that of other neuronal subtypes 55

Figure 15: Loss of β-cells in RIP-cmyc^{ER} mice appears to have an intermediate effect on parasympathetic islet innervation 56

Figure 16: A preliminary comparative analysis of autonomic innervation in the non-obese diabetic (NOD) and the NOD/RAG mouse 61

Chapter 1: Introduction and Background

Introduction

There are three neuron types—sympathetic, parasympathetic, and sensory— that innervate the pancreas, in addition to an astroglial population. The sympathetic and parasympathetic branches of the autonomic nervous system are involved in maintenance of blood glucose homeostasis in response to changing energy demands. Sympathetic neurons mediate the so-called "fight or flight" response through stress-induced neural activity. They inhibit insulin secretion and up-regulate glucagon release by respective β- and α-cell populations in the pancreatic islets of Langerhans, the net physiological result of which is to convert glycogen stores to blood glucose to meet immediate energy demands. Through feeding-induced neural activity, parasympathetic neurons stimulate insulin secretion from insulin-producing β-cells to promote the removal of glucose from the blood into the liver for storage as glycogen, while repressing glucagon release (Ahren 2000). Sensory neurons are involved in pain sensation; indeed, extreme pain is a well-documented concern in pancreatitis and pancreatic cancer patients (Wick et al. 2006a, 2006b). The function of pancreatic astroglia, which encapsulate the islets of Langerhans, is not definitively known, although there is increasing evidence that astroglia are involved in synaptic transmission in the brain, and thus may be more involved in neuronal signaling than previously speculated (Halassa et al. 2007).

Anatomical and physiological characteristics of the pancreas pose technical challenges to the study of innervation. Many antigens that are considered dependable neural markers within the CNS are unsuitable for use in the pancreas because various pancreatic endocrine cells also display them. Furthermore, due to the irregular

morphology of islets and the network of neurons that innervate them, thin-section immunofluorescence techniques miss important 3-dimensional information. Thus, previous developmental studies have been limited in their ability to distinguish between specific pancreatic nerve populations, and to obtain high-resolution images (Yokoyama et al. 2002; Persson-Sjogren et al. 2005). This has hamstrung the ability to obtain specific information regarding when particular neuronal and astroglial cell types arrive in the developing pancreatic bud, as well as temporal information concerning the development of pancreatic neurons-- the elongation of neural fibers as well as the formation of neuro-endocrine contacts-- in the context of pancreatic development. In this study we employ confocal fluorescence microscopy, using neuronal subtype-specific antibodies on thick sections at particular stages in embryonic development, postnatal maturation, and in the context of synthetic pancreatic disease, to gain a greater understanding of the neuronal and glial populations associated with the pancreatic islets.

The mature pancreas is a dynamic organ; old endocrine cells die and new cells are born while endocrine innervation is maintained throughout the life of the organism. Pancreatic innervation is being viewed with increasing interest with respect to pancreatic diseases, yet relatively little is known about pancreatic innervation during development and disease (Saravia and Homo-Delarche 2003; Konturek et al. 2003; Yi et al. 2003; Persson-Sjogren et al. 2001; Rossi et al. 2005; Lindsay et al. 2006). Nonetheless, pancreatic nerves have recently been identified as a possible early target population in autoimmune diabetes, and there is increasing evidence that neuroendocrine remodeling does take place in the pancreatic islets of diabetic disease models (Saravia and Homo-Delarche 2003; Winer et al. 2003; Persson-Sjogren et al. 2005). There is also growing

evidence for the innervation of transplanted islets, as multiple neuronal markers are present in islets post-transplantation (Persson-Sjogren et al. 1998; Persson-Sjogren et al. 2002)

One goal of the present study was to perform a descriptive analysis of the growth and development of sympathetic and sensory neurons and astroglia during pancreatic organogenesis and maturation. In addition, we aimed to assay a synthetic pancreatic disease model for subtype-specific effects of large-scale β-cell loss and repopulation on the maintenance of islet innervation. To accomplish these goals we performed confocal analysis using single, double, and triple labeling immunohistochemistry. We included embryonic, neonatal, adolescent and adult wild-type mice in our developmental study. We also took advantage of the recent development of the RIP-cmyc^{ER} line, a transgenic mouse line that conditionally expresses cmyc specifically in β-cells. This enabled us to orchestrate the death and subsequent resurgence of this subpopulation of endocrine cells (Pelengaris et al. 2002). We used the RIP-cmyc^{ER} regeneration model to determine the effect on existing pancreatic neurons when the bulk of β-cells are ablated and replenished.

In contrast to previous research, this analysis concerns itself with the relationship of specific neural and glial pancreatic subpopulations to both the developing and mature endocrine pancreas. It explores these populations, at the level attainable by confocal fluorescent microscopy, in order to address both developmental and maturational aspects of islet innervation in the wild type mouse, as well as disease-related aspects of innervation maintenance in a synthetic adult disease model. We report that the sympathetic and sensory populations appear in the developing embryonic pancreas in a

temporally discrete fashion. We show that islet innervation by distinct cell types is temporally integrated with the intrapancreatic endocrine cell migration and organization that characterize pancreatic embryonic development and postnatal maturation, respectively. Finally, we observe that the sympathetic, sensory and astroglial populations in the pancreas are affected differently by depletion and restoration of the β-cell population in RIP-cmyc^{ER} mice.

Background: Pancreatic Morphology and Organogenesis

The pancreas is positioned in the center of the gut, with the dorsal pancreas situated between the stomach and spleen, and the ventral pancreas nestled into the first loop of the duodenum. It is comprised of both exocrine and endocrine components, and is central to many vertebrate functions, including digestion, maintenance of blood glucose homeostasis, regulation of energetic stores in relation to changing energetic needs, feeding behavior, and satiety cues. Only ~1% of the pancreas is comprised of endocrine cells, which are stereotypically arranged throughout the organ into clusters known as the islets of Langerhans. The islets themselves consist of a core cluster of insulin-producing β-cells, which are surrounded by a peripheral assortment of glucagon-producing α-cells, somatostatin-producing δ-cells, pancreatic peptide (PP) cells, and ghrelin-producing cells.

Pancreatic organogenesis is initiated at roughly embryonic day 8 (E8). Physical contact between the notochord and the embryonic ectoderm produces developmental signals central to gut development (Figure 1A). Evagination of the pancreatic buds marks the beginning of early pancreatic morphogenesis, which begins around E10 and

continues through E13. The dorsal pancreatic bud begins to evaginate from the anterior small intestine just caudal to the stomach, closely followed by outgrowth of the ventral pancreatic bud (Figure 1B). Pancreatic tissue proliferation, endocrine cell type specification and nascent islet formation all take place during embryonic morphogenesis.

In the mouse, the pancreas undergoes a period of postnatal maturation that lasts for about four weeks after birth (Figure 1C). At postnatal day 0 (p0), endocrine cells may be found scattered or clustered throughout the pancreas, as nascent islets are still being formed. Unaffiliated endocrine cells migrate to join islet clusters until adulthood is reached.

Background: Neural Crest Development

The process of pancreatic innervation is one facet of pancreatic organogenesis about which little is known. Multiple neural and astroglial cell types infiltrate or project into the pancreas during embryonic organogenesis, forming neuro-pancreatic connections that are necessary to the proper mediation of pancreatic function.

Development of the neural crest, from which pancreatic neurons are derived, begins with the process of neurulation (Graham 2003). Formation of the neural tube brings together two neural folds that are formed at the interface between the neural plate and the epidermal ectoderm. These folds form the dorsal aspect of the neural tube, and the neural crest. Once neural crest cells have been specified, they undergo an epithelial to mesenchymal transition and delaminate from the neural tube. Neural crest cells migrate away from the midline dorsal to the neural tube, toward the somites' anterior; they are excluded from the somites' posterior (Figure 3A). This migration takes place in

three distinct waves that result in the positioning of neural crest cells in distinctly separate areas (Figure 3B). The earliest migrating crest cells travel ventrally to the vicinity of the dorsal aorta, and give rise to the cells of the sympathetic ganglion. The second wave terminates in the anterior half sclerotome of each somite to generate the dorsal root ganglion and sensory neurons. Late migrating crest cells migrate dorsolaterally just beneath the ectoderm, forming melanocytes (Graham 2003; Bronner-Fraser 1993).

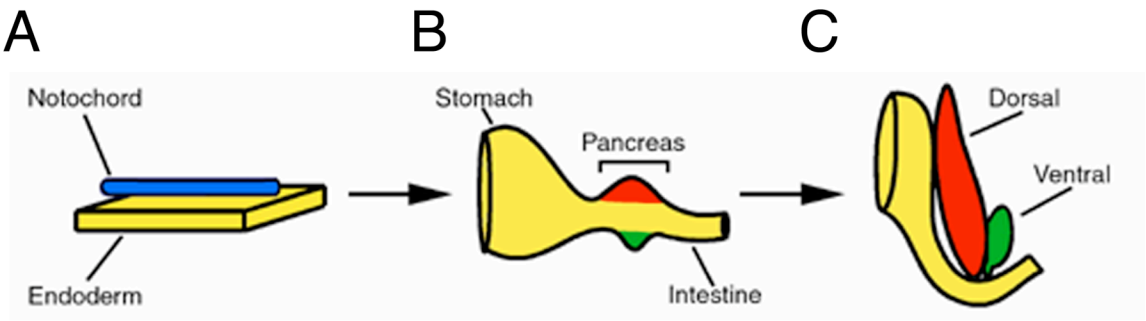


Figure 1: The stages of pancreatic organogenesis and maturation. Pancreatic organogenesis is initiated at roughly embryonic day 8 (E8) by developmental signals that are produced by contact between the notochord (blue) and the embryonic ectoderm (yellow, A). Early morphogenesis takes place between E10 and E13, as dorsal and ventral pancreatic buds (red and green, respectively) evaginate from the anterior small intestine just caudal to the stomach (B). The dorsal and ventral pancreas (red and green, respectively) continue to grow during a period of postnatal maturation that lasts from birth through approximately 4 weeks of age (C). *Borrowed from M. Hebrok.*

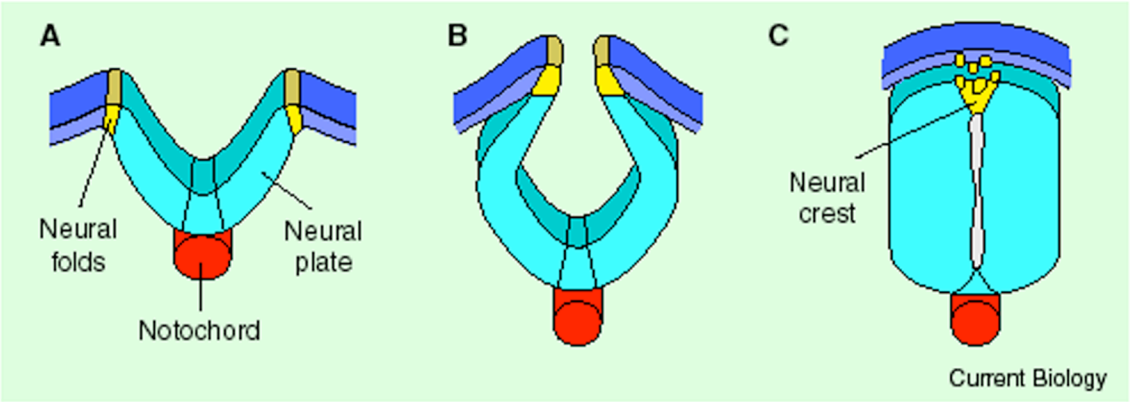


Figure 2: Development of the neural crest begins with the process of neurulation. The neural plate (light blue) progressively folds to form the neural tube (A). Neural folds (yellow) form at the interface between the neural plate and the epidermal ectoderm (dark blue), and progressively come together (B) to form the dorsal aspect of the neural tube and the neural crest (yellow, C). *Adapted from A. Graham, 2003.*

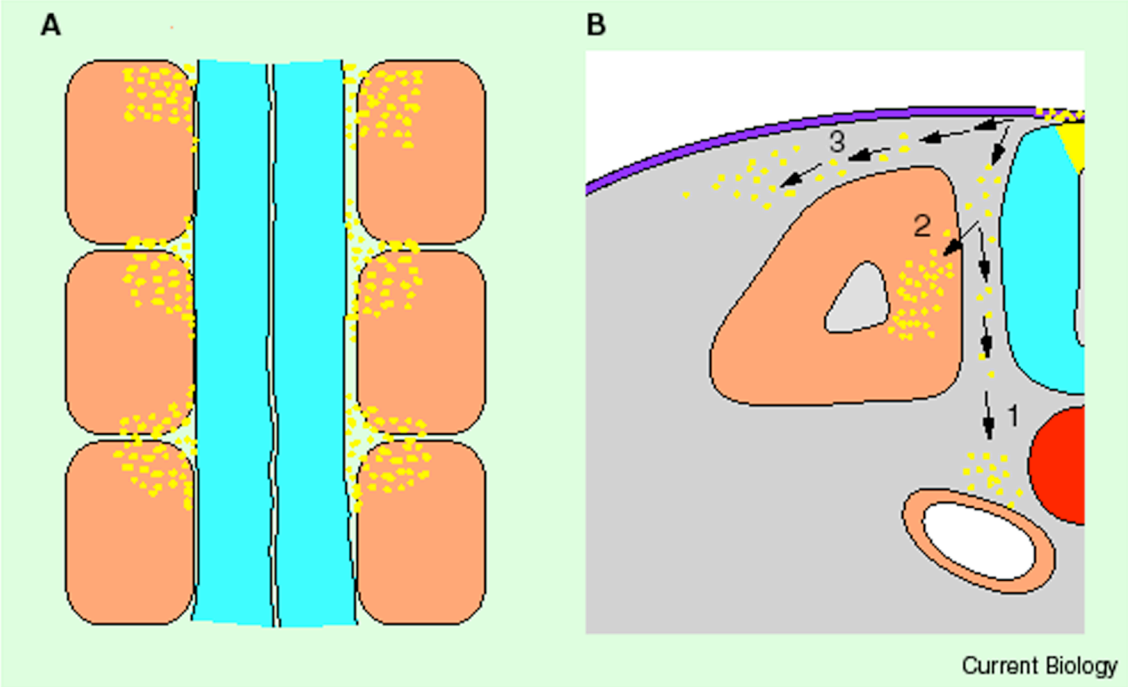


Figure 3: Migration of the trunk neural crest occurs in three temporally and positionally distinct waves. Neural crest cells migrate away from the midline dorsal to the neural tube (blue), toward the somites' anterior (A). The earliest migrating crest cells travel ventrally (B1) to give rise to the cells of the sympathetic ganglion. The second wave (B2) enters the anterior sclerotome to generate the dorsal root ganglion. Late migrating crest cells (B3) form melanocytes. *Adapted from A. Graham, 2003.*

Chapter 2: Methods

Experimental Animals

Developmental experiments were performed on embryonic (e9.5-18.5), neonatal (p0-p7), adolescent (p10-28) and adult (3-6 month) wild type CD1 mice, as well as neonatal (p0-p7) Pax4-Shh transgenic mice (C57BL/6) transgenic mice. Synthetic hyperglycemia and recovery experiments were conducted on RIP-cmyc^{ER}/+ (C57BL/6) experimental mice and wild type littermate controls, aged 8-10 weeks at the beginning of tamoxifen administration. For prenatal analysis, 4-10 wild type CD1 embryos were analyzed per stage; for postnatal analysis, 5-8 wild type CD1 animals were analyzed per stage; for RIP-cmyc^{ER} islet regeneration analysis, 4-5 RIP-cmyc^{ER}/+ experimental animals and 4 control animals were analyzed per stage. Males and females were represented in roughly equal proportions in all experimental groups. All experimental results were confirmed in duplicate or triplicate. The mice were housed in accordance with NIH guidelines and kept in a facility maintained at 22°C with an alternating 12h light/dark cycle. Mice were given standard mouse chow and water *ad libitum*. All procedures were approved by the Institutional Animal Care and Use Committee at the University of California, and were conducted in accordance with NIH and UCSF LARC guidelines.

Tissue preparation and immunofluorescent processing

Pancreata were isolated from wild type CD1 mice ranging from 12.5 days post coitus through 6 months in age and fixed 2-16 hours at 4°C in zinc-buffered formalin fixative (Anatech). Whole embryos ranging in age from e10.5-15.5 were fixed up to 16

hours at 4°C in zinc-buffered formalin fixative, after which they were either treated as whole mount tissues or pancreata were excised from the fixed embryos for cryoprotection. After fixation, tissues were cryoprotected 16 hours in 30% sucrose in 0.1M PBS at 4°C, then immersed in TissueTek (Sakura, Torrance, CA USA) in peel-away molds and frozen in an ethanol/dry ice bath. Tissue blocks were stored at -80°C. Tissue sections were cut on a cryostat at a thickness of 50μm. Serial sections were thaw mounted and affixed to glass slides before staining.

Relative thickness of the tissue sections dictated that the protocol for immunofluorescence preparation would be lengthier than the protocols normally in use for thin (typically 0.5-1μm) sections. Extra time was allotted in the devised protocol for the permeabilizing, blocking, and washing of samples. Sections were air dried at room temperature for 90 minutes to affix tissue to glass slides. Section samples were incubated for 90 minutes in 0.3% Triton X-100 in 1× PBS to dissolve TissueTek. Triton X-100 detergent was included in solutions during subsequent steps to aid in permeabilization of the tissue. Samples were next incubated in blocking buffer consisting of 0.3% Triton X-100, 4% BSA, and 0.02% NaN_3 in 1× PBS at 4°C 16 hours. Primary antibodies were diluted in diluent buffer consisting of 0.3% Triton X-100, 4% BSA in 1× PBS and applied to sections (see Table 1 for antibodies and conditions employed). Sections were rinsed 4× quickly and washed 6×1 hour at room temperature in wash solution consisting of 0.3% Triton X-100 in 1× PBS, and blocked 16 hours in blocking buffer at 4°C before being treated with fluorescently labeled secondary antibodies. Secondary antibodies were diluted in diluent buffer as described above and applied to sections (see Table 1), then rinsed 4× quickly and washed 6×1 hour at room temperature in wash solution as

described above. Sections were rinsed 3×5 minutes in PBS, mounted with Vectashield + DAPI or Vectashield Hard Set + DAPI (Vector Labs) and imaged.

RIP-cmyc^{ER} activation protocol

The RIP-cmyc^{ER} line is a transgenic mouse line, in which the gene *cmyc* is expressed under the control of the rat insulin promoter (RIP). Expression of the transgene in pancreatic β-cells is induced by the intraperitoneal administration of tamoxifen, and ceases when tamoxifen administration is stopped (Pelengaris et al. 2002). All mice used in these experiments were 8-10 weeks of age at the beginning of the tamoxifen administration protocol. Both male and female animals were used in roughly equal proportion.

Tamoxifen (Sigma T5648) was dissolved 10 mg/mL in corn oil and 1mg (100μl) was injected intraperitoneally into experimental mice once every 24 hours +/- 1 hour for 6 days. Control mice were injected with vehicle alone. Ascensia Elite blood glucose monitors and test strips (Bayer) were used to monitor non-fasting blood glucose. Non-fasting blood glucose was measured on days 3 and 7 of the tamoxifen regime, as well as at the time of sacrifice for all mice (days 9, 11, 13, 23, 30, 45, and 60 post initiation of tamoxifen administration).

Mice were considered hyperglycemic if blood glucose ≥ 200 mg/dL on day 7; blood glucose of all transgenic mice assayed was ≥350 mg/dL by day 7. Control animals had blood glucose levels below 200 mg/dL at day 7. Pancreata were harvested on test/sacrifice dates, and tissues were fixed and prepared for cryosection as above.

Pancreata were sectioned into 50μm sections and affixed to glass slides before staining. The immunofluorescence staining protocol was conducted as described above.

Immunofluorescent confocal microscopy

Confocal images were taken using Leica DMRE SL and SP2 confocal microscopes and Leica confocal software. Images were obtained with 20x and 40x oil immersion lenses, and the microscopes were equipped with optical zoom capability. For 2-dimensional composite images, at least 1 confocal image was taken per micron of tissue thickness. Images were processed and contrast and brightness were adjusted using Adobe Photoshop.

Attempted direct fluorescent labeling of primary antibodies

A large number of antibodies raised against many neural and synaptic markers were tested for use in this analysis. It was found that all the primary antibodies that proved amenable to being used to visualize pancreatic nerves were rabbit polyclonal antibodies. As such, it was not possible to perform co-stains using VMAT2, CGRP, and GFAP simultaneously. In an effort to make the simultaneous visualization of multiple neural subtypes possible, primary antibodies were directly fluorescently labeled using the Zenon kit (Invitrogen). The labeling was conducted as described in the kit directions, and appeared to be successful. However, direct fluorescent labeling of the neural proteins listed did not provide enough fluorescence for proper confocal analysis. It is likely that the antigens under study are present at levels that require the amplification provided by use of secondary labeled antibodies, and therefore are not amenable to being viewed by

direct labeling of primary antibodies. Thus simultaneous labeling of multiple neural and astroglial subtypes was not included in this analysis.

Vibratome section preparation

In the course of determining the optimal thickness for tissue sections, I attempted to utilize vibratome sectioning. The aim of this was to obtain sections 100-200μm in thickness, in hopes of being able to fully render the morphology of pancreatic islets and islet innervation in three dimensions. Adult pancreata were obtained and fixed as outlined above, and then embedded in low-melting-point agarose (Gibco BRL). The resulting tissue blocks were then cut on a Leica VT1000S vibratome to various thicknesses and prepared for fluorescence imaging as above. It was determined that sections over 50μm in thickness were not amenable to staining and confocal analysis, owing to difficulties in tissue permeability by antibodies. As tissues 50μm thick could be more easily and reliably obtained through use of a cryotome, vibratome sectioning was deemed unnecessary to this analysis.

Chapter 3: Results

Innervation morphology of the adult pancreatic islet

Antibodies recognizing vesicular monoamine transporter 2 (VMAT2), calcitonin gene-related peptide (CGRP), and glial fibrillary acid protein (GFAP) were used to visualize postganglionic sympathetic neuronal processes, sensory neuronal fibers, and pancreatic astroglia, respectively. $VMAT2^+$ staining was occasionally observed in adult β-cells as has previously been reported, though at a relatively low level and in a diffuse cytoplasmic pattern that was easily distinguishable from the bright vesicular reactivity observed in $VMAT2^+$ neurons (Anlauf et al. 2003; Weihe and Eiden 2000). $VMAT2^+$ staining was not observed in α-, δ-, or PP-cells in the endocrine pancreas; CGRP reactivity was observed only in $CGRP^+$ neurons; and GFAP reactivity was specific to pancreatic astroglia.

In adult mice, $VMAT2^+$ sympathetic and $CGRP^+$ sensory fibers entered pancreatic islets at multiple points. Neural fibers were enriched at the islet periphery, although occasional detection of fibers within islet cores indicates that they are not necessarily excluded from the inside of the islets (Figure 4A, B, D and E). $GFAP^+$ astroglia were highly associated with the islet periphery as they encapsulated pancreatic islets (Figure 4C, F).

Sympathetic ($VMAT2^+$) neuronal fibers were quite distinct in the extent of their perivascular association in the adult mouse. Multiple $VMAT2^+$ sympathetic tracts form an elaborate perivascular plexus around large and medium-sized pancreatic blood vessels as visualized with an antibody recognizing mouse pan-endothelial cell antigen (MECA32) (Figure 5A). Sympathetic capillary association was also occasionally

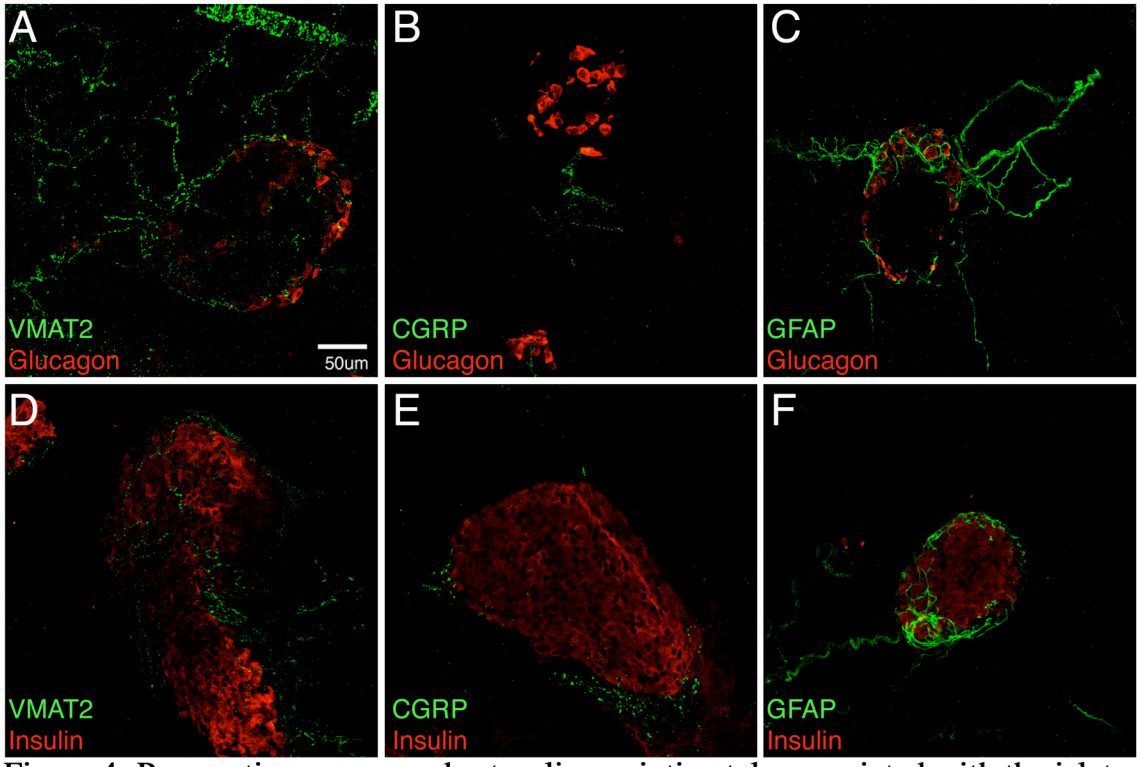


Figure 4: Pancreatic neurons and astroglia are intimately associated with the islets of Langerhans. Sympathetic and sensory neurons, as well as astroglia (green), all populate pancreatic islets. Sympathetic and sensory neural fibers appear concentrated at the islet periphery defined by glucagon-producing α-cells (red, A-C), relative to the islet core defined by insulin-producing β-cells (red, D-F). N=8. Scale bar=50μm

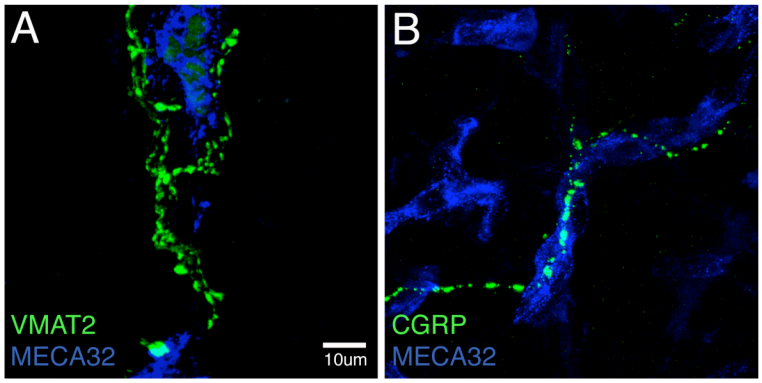


Figure 5: Adult pancreatic neural processes have distinct modes of perivascular association. Sympathetic fibers (green, A) are highly fasciculated relative to sensory fibers, and form an elaborate perivascular plexus that surrounds large and medium-sized blood vessels (blue, A). Sensory fibers (green, B) are somewhat less fasciculated, and tend to align with the vasculature (blue, B). N=8. Scale bar=10μm

detectable within islets (data not shown). Sensory fibers were no less elaborate than autonomic fibers, although $CGRP^+$ tracts tended to align longitudinally with blood vessels, without forming plexuses (Figure 5B). None of the populations assessed were found to associate closely with pancreatic duct architecture (data not shown).

Sympathetic and sensory neurons enter the pancreatic bud during late embryogenesis (e10.5-e18.5)

Evagination of the mouse dorsal pancreatic bud is known to initiate at embryonic day 9.5 (e9.5) and pancreatic tissue continues to proliferate throughout embryonic development (Kim and Hebrok 2001). To delineate the pattern of innervation during embryonic development, we began the analysis of tissue at e10.5 and continued to e18.5, just preceding birth. Staining of sagittal sections from e10.5 whole-mount embryos detected a $VMAT2^+$ cell population present as a streak of cells along the length of the neural tube (Figure 6A). No $VMAT2^+$ cell bodies were detected in the pancreatic bud at e10.5. The earliest presence of $VMAT2^+$ cell bodies was detected at e12.5 in excised pancreatic tissue (Figure 6B). $VMAT2^+$ cell bodies were detected just inside the pancreatic periphery, indicating that e12.5 is probably the earliest point at which $VMAT2^+$ cell bodies enter the pancreatic bud. $VMAT2^+$ neuronal fibers were not detected in embryonic pancreatic tissues (Figure 6C).

CGRP was present at very low levels in individual sensory cell bodies along the neural tube at e10.5 (Figure 6D). By e12.5, a small number of single $CGRP^+$ cell bodies were detected in excised pancreatic bud tissue, indicating that $CGRP^+$ cells may first enter the pancreas at this stage in concert with $VMAT2^+$ cells (Figure 6B, E). CGRP was

detected more strongly after sensory precursors entered the pancreatic bud, and by e15.5 $CGRP^{+}$ sensory fibers were highly elaborate (Figure 6F).

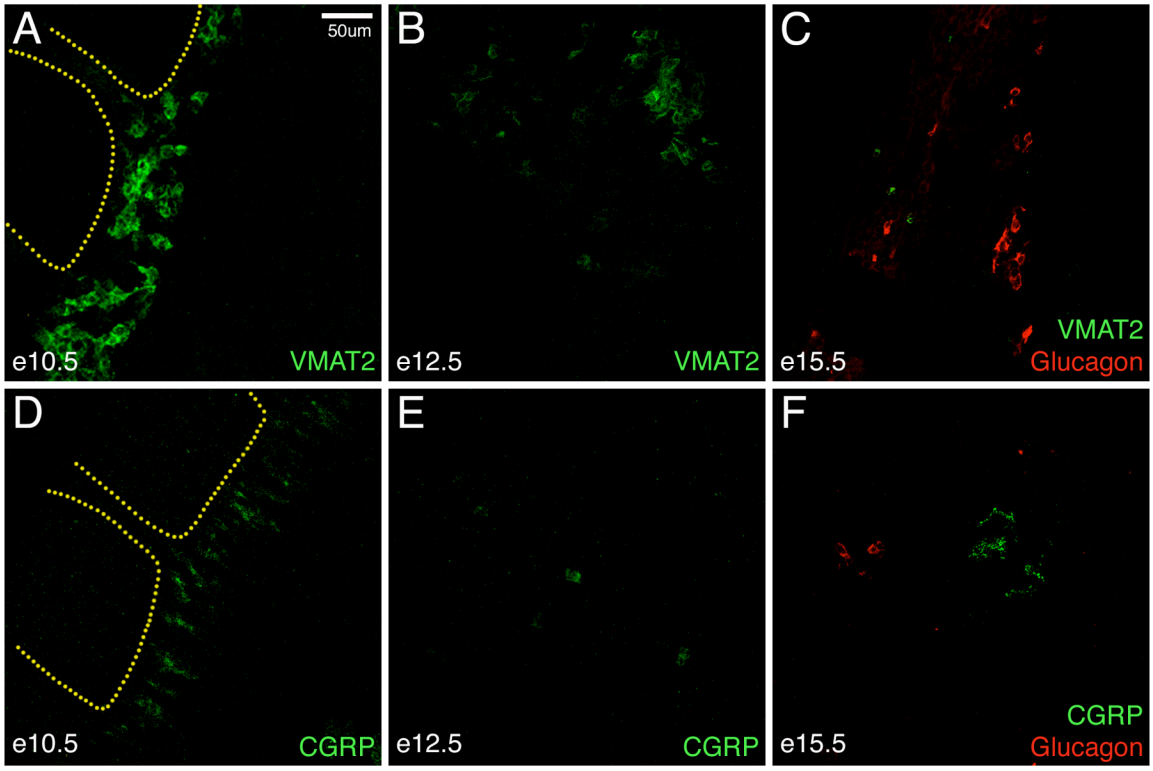


Figure 6: Sympathetic and sensory cell bodies enter the pancreatic bud during organogenesis. At embryonic day 10.5 (e10.5), the sympathetic VMAT2$^+$ cell population is visible along the neural tube of a sagittally sectioned whole mount (green, A; somites are outlined in yellow). No VMAT2$^+$ cell bodies are seen in the pancreatic bud at this time (N=10). Sensory CGRP$^+$ cell bodies are also detected along the neural tube at e10.5 (green, D), but are morphologically distinct from VMAT2$^+$ cells (N=8). VMAT2$^+$ and CGRP$^+$ cells are first detected in the excised pancreas at e12.5; CGRP$^+$ cells are detected in much lower numbers than VMAT2$^+$ cells in e12.5 (N=4) pancreas (green, B and E). In the e15.5 (N=5) pancreas, VMAT2 is still confined to sympathetic cell bodies, while CGRP is detected in elaborate neural fibers (C, F). Tangential edges of cell bodies are occasionally depicted (white arrowheads, C and F). Scale bar=50μm

Islet innervation and encapsulation take place coincident with postnatal islet maturation (p0-21)

Sympathetic innervation

The postnatal maturation of $VMAT2^+$ sympathetic neural fibers can be described in terms of the changing nature of their contact with endocrine cells and blood vessels during development. At birth, endocrine cells may be found scattered or clustered throughout the pancreas, and $VMAT2^+$ cell bodies are detected among scattered endocrine cells (Figure 7A). Unaffiliated endocrine cells migrate to join islet clusters until adulthood is reached. Adult islets have a characteristic arrangement of endocrine cells: β-cells are found at the islet core, surrounded by α-, δ- and PP cells (Kim and Hebrok 2001).

$VMAT2^+$ fibers could be seen closely associated with endocrine cells during the first postnatal week, long before endocrine cell migration and islet formation have been completed (Figure 7B). During the second postnatal week, α- and β-cells continue their migration in the course of adopting the mature islet configuration. Sympathetic islet innervation remained largely concentrated at the periphery of the maturing islets, and closely resembled the adult configuration by p15 (Figure 7B, C).

At p4 $VMAT2^+$ neural fibers were often observed in absence of associated blood vessels (Figure 8A). This appeared unique to the first postnatal week, as by p7 the incipient perivascular plexus began to be clearly visible on larger vessels (Figure 8B). Perivascular association of sympathetic fibers increased in complexity during the second postnatal week. The incipient plexus formation that was first visible at p7 reached a level

of elaboration characteristic of the adult sympathetic perivascular plexus by p15 (Figure 8C).

Sensory Innervation

As in the case of sympathetic nerves, association of sensory fibers with endocrine cells takes place during the early processes of endocrine migration and islet formation. By p0, $CGRP^+$ fibers were closely associated with endocrine cells in many nascent pancreatic islets (Figure 7D). $CGRP^+$ fibers themselves did not change appreciably between p0 and p7; by the beginning of the second postnatal week, as endocrine cells coalesced into islets, $CGRP^+$ fibers became clearly visible at the periphery of islets (Figure 7E). $CGRP^+$ innervation remained largely concentrated at the periphery of islets throughout the maturation process. Thus sensory-endocrine association at p15 closely resembled that found in adult islets (Figure 7F).

Astroglial Encapsulation

GFAP is not detectable in astroglia before p6 (Figure 7G); this precludes its use to track the presence of astroglia in mouse embryos and neonates. Faintly GFAP-reactive cells were first visible at p6, after nascent pancreatic islets have begun to form but long before islet maturation is considered complete. At this stage, $GFAP^+$ cells came into close contact with glucagon-producing cells at the islets' periphery. At p6, $GFAP^+$ cells were also in contact with endocrine cells that had yet to become clearly affiliated with islets (data not shown). By p7, the beginning of the second postnatal week, rudimentary $GFAP^+$ encapsulation of the maturing islets was evident (Figure 7H). The amount of $GFAP^+$

encapsulation increased as pancreatic islets continued to mature, and by p15 astroglial encapsulation of islets closely resembled the adult morphology (Figure 7I).

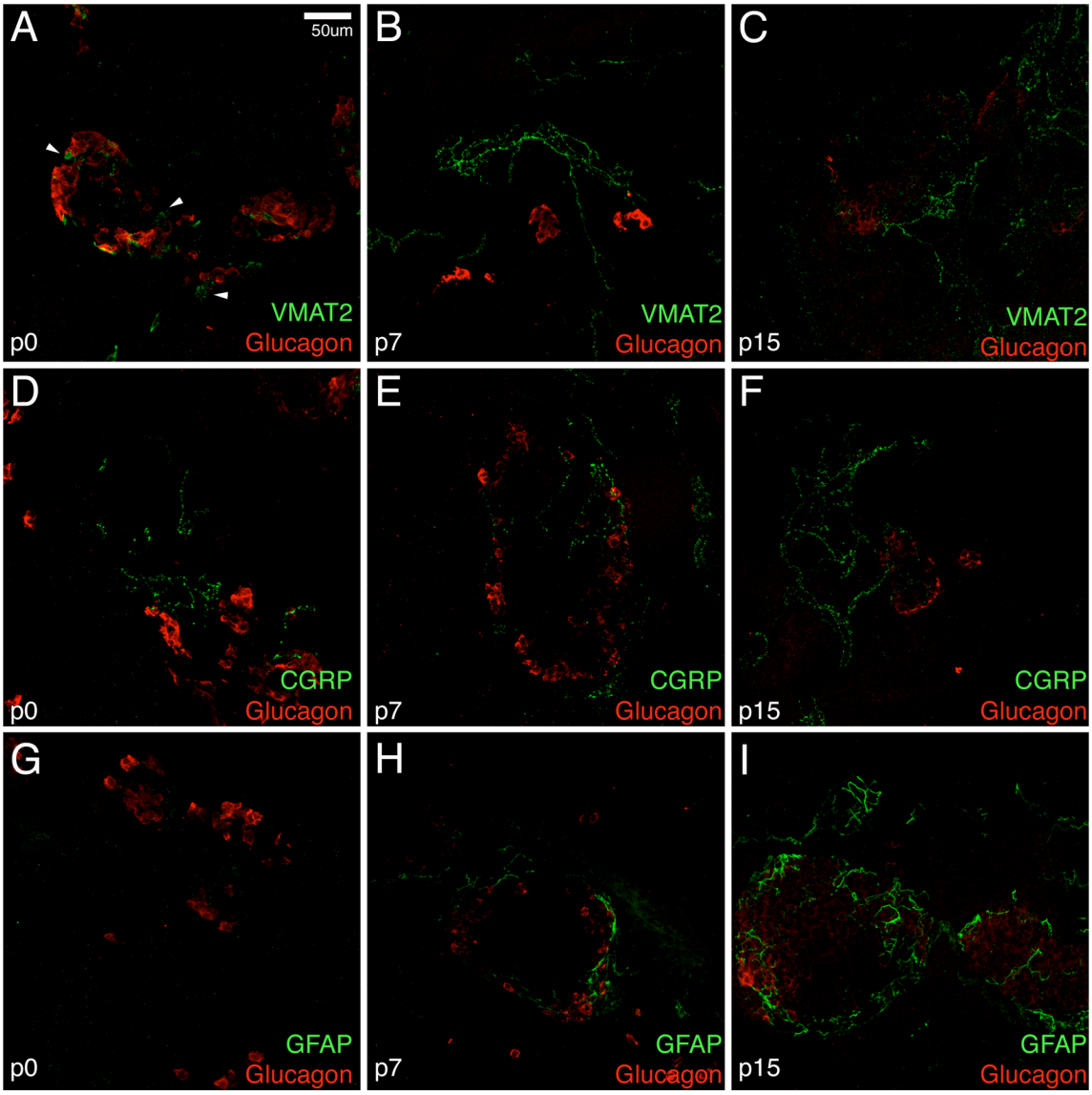


Figure 7: Nerve growth and islet innervation during postnatal pancreatic maturation p0-p15. Sympathetic cell bodies (green, white arrowheads) are interspersed with endocrine cells (red) at birth (A; N=5), as endocrine cells are still migrating to form nascent islets; VMAT2^{+} fibers become more elaborate as islets begin to adopt their mature configuration (B; N=5), but tend to remain concentrated at the periphery of the maturing islets (C; N=4). Sensory fibers become associated with glucagon-producing α-cells as early as p0 (D; N=5); as with sympathetic fibers, sensory nerves follow islet capillaries (E), but remain enriched at the islet periphery throughout islet maturation (E, F; N=5 for each). GFAP is not a viable marker at birth (G; N=7), but astroglial encapsulation of nascent islets is under way by p7 (H; N=4), and increases as islets mature (I; N=4). Scale bar=50μm

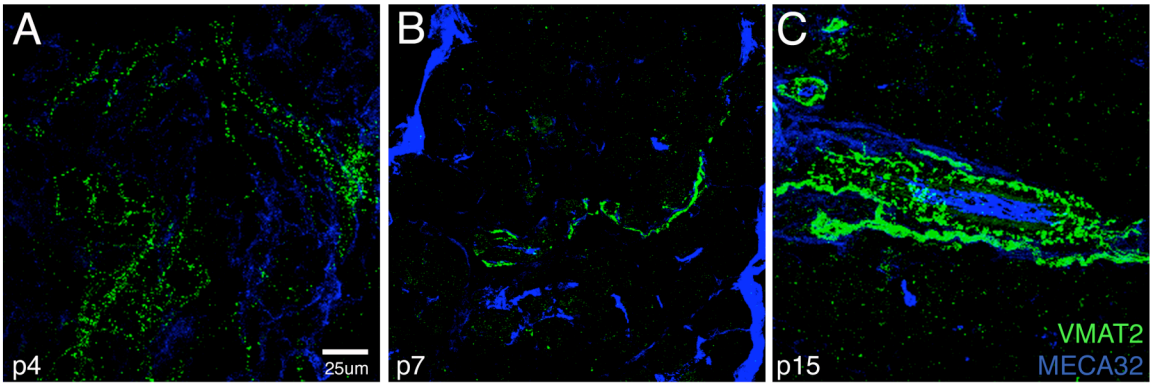


Figure 8: Growth of the sympathetic perivascular plexus during postnatal pancreas maturation. VMAT2^{+} fibers (green) associate with blood vessels (blue) by p4, but occasionally depart from the vasculature (A; N=4). Initial perivascular plexus formation is detected at p7 (B; N=5). Vascular association resembles the adult perivascular plexus by p15 (C; N=4). Scale bar=25μm

Selective loss of β-cells differentially affects maintenance of islet innervation in RIP-cmyc^{ER} mice

We used the RIP-cmyc^{ER} regeneration model to determine the effect on existing neurons and neuroendocrine connections when the bulk of β-cells are ablated and replenished. As the β-cell population declines, mice quickly become hyperglycemic; they recover normal blood glucose levels as the islets are repopulated with β-cells over a two-month period. As such, this mouse line provides a β-cell regeneration model in which to study the maintenance of endocrine innervation during the course of β-cell loss and recovery (D. Cano and P. Heiser, personal communications).

RIP-cmyc^{ER} mice were treated with a 6-day course of intraperitoneal tamoxifen injection, monitored for changes in blood glucose, and sacrificed for tissue preparation as described above. Mice were clearly hyperglycemic, with a mean non-fasted blood glucose levels exceeding 400 dl/ml at day 3 of cmyc induction, compared to under 200 dl/ml in untreated controls; animals began to recover normoglycemia shortly after cessation of cmyc induction, and blood glucose levels returned to normal range by 60 days after cmyc induction (Figure 9). Mice were observed to have similar blood glucose levels at similar points along the recovery trajectory, regardless of sex. No sexual dimorphism was observed with regard to the expression patterns detailed below.

Loss of β-cells is sufficient to cause pancreas-wide delocalization of a monoamine transporter in post-ganglionic sympathetic nerves

Pancreata harvested 7 days post-initiation (dpi) of cmyc activation were found to lack VMAT2^{+} reactivity, a marker of sympathetic innervation (Figure 10B). The loss of

sympathetic VMAT2 was homogeneous throughout the pancreas. By 13dpi (1 week after cmyc activation has been discontinued), VMAT2 had begun to reappear in perivascular sympathetic fibers. Low levels of VMAT2 were detectable in a pattern characteristic of the sympathetic perivascular plexus, but sympathetic VMAT2 reactivity remained absent around pancreatic islets (Figure 10C). At roughly 30dpi, VMAT2 was observed in islet-associated sympathetic fibers, and VMAT2 reactivity in perivascular fibers closely resembled that of wild type animals; VMAT2 appeared to be largely recovered in islet-associated fibers by 60dpi (Figure 10D). Overall, the recovery of VMAT2 reactivity in pancreatic sympathetic nerve fibers coincided temporally with the repopulation of islets with beta cells, and with recovery of normoglycemia as measured by blood glucose tests (Figure 10A-D).

To more closely determine the extent of disruption in postganglionic sympathetic neurons, RIP-cmyc^{ER} specimens were also stained with antibodies to detect the presence of neuropeptide Y (NPY), a modulator of glucagon secretion that is also present in postganglionic sympathetic neurons (Adeghate 2002). NPY was present throughout the loss and resurgence of β-cells, indicating that although VMAT2 localization was disrupted, the architecture of postganglionic sympathetic neurons was intact (Figure 11). Thus, we conclude that large-scale β–cell loss alone is sufficient to disrupt VMAT2 localization, but insufficient to disrupt the structure of sympathetic neurons in the pancreas.

Large-scale β-cell loss has a delayed and transient effect on astroglial-endocrine association

The effect of large-scale β-cell depletion on pancreatic astroglia was both subtle and delayed relative to its effects on the sympathetic nerve population. Astroglial association with islets visualized at 7dpi and 9dpi did not appear decreased relative to controls (Figure 10E, F). However, astroglial encapsulation of pancreatic islets was visibly lessened by 13dpi (Figure 10G). Thus we surmise that the decrease in astroglial-islet association occured after, rather than during, the initial loss of β-cells. This decrease appeared to be transient, as islet encapsulation at 60 days post cmyc activation looked very similar in extent to encapsulation in wild type animals (Figure 10H). It should be noted that, in contrast to the case of sympathetic neural fibers, the observed decrease in astroglial islet encapsulation was not characterized by a loss in astroglial GFAP reactivity. Remaining $GFAP^{+}$ cells were still clearly associated with islets, and appeared to be healthy.

Islet sensory innervation appears unaffected in RIP-cmyc^{ER} mice

In contrast to the demonstrated effects of large-scale β-cell depletion on sympathetic neurons, no readily apparent interruption of sensory innervation of pancreatic islets was revealed in RIP-cmyc^{ER} mice. CGRP reactivity was detected and resembled wild type reactivity at 7dpi and 9dpi; the same was true of tissues from animals isolated at 60dpi (Figure 10I-K). No morphological changes were detected in sensory neurons at islets throughout stages of β-cell repopulation.

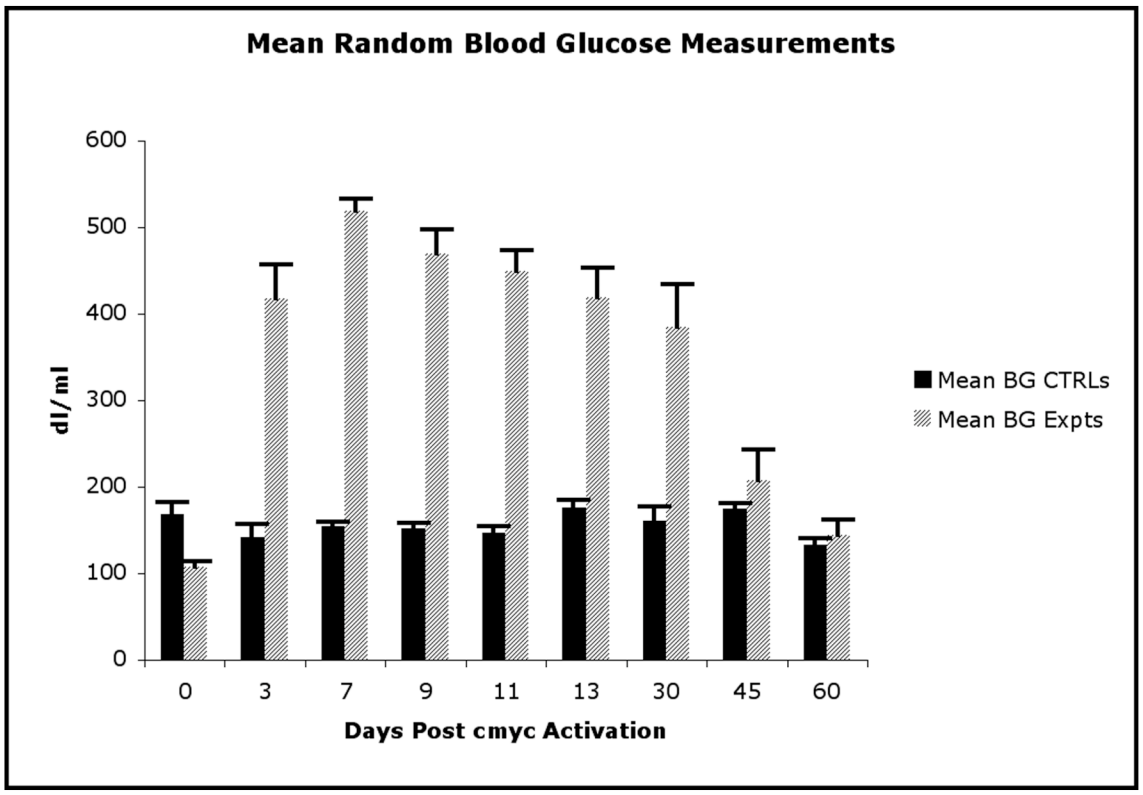


Figure 9: Induction of hyperglycemia is followed by recovery of normoglycemia in RIP-cmyc^{ER} mice. By 3 days post initiation (dpi) of tamoxifen injections, the mean blood glucose of RIP-cmyc^{ER} animals is 417.42dl/ml (N=21), compared to 141.33dl/ml in control mice (N=6). Difference between the two cohorts reaches a maximum of 365.14dl/ml at 7dpi. Mean blood glucose begins to decline shortly after discontinuation of tamoxifen, and reaches the control range by 60dpi.

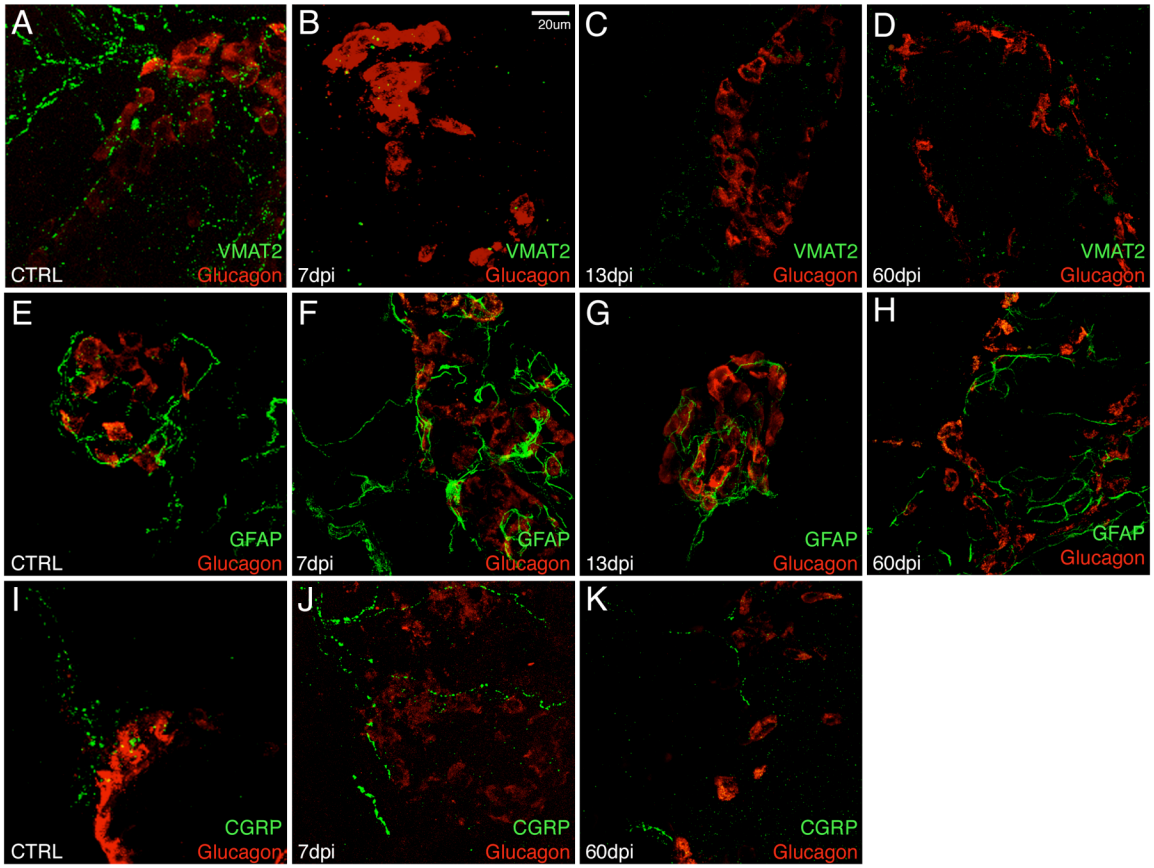


Figure 10: Differential effects of β-cell loss on sympathetic and sensory neurons and astroglia. VMAT2-reactivity in sympathetic fibers (green, A-C) was lost by 7dpi (A) and restored during the next 7 weeks (B, C) of β-cell recovery in RIP-cmyc^{ER} mice. Fluctuations in the β-cell population resulted in a transient decrease in GFAP^{+} islet-associated astroglia (green, D-F). Although overall GFAP-reactivity did not seem to be affected, the degree of astroglial surround of islets had declined markedly by 2 weeks following initiation of cmyc activation in β-cells (E). Islet encapsulation increased over the following 6 weeks to become indistinguishable from wild type (F). CGRP-reactivity in sensory fibers (green, G and H) was retained in islets during the same time frame. Control N=4; 7dpi N=4; 13dpi N=5; 60dpi N=5. Scale bar=20μm

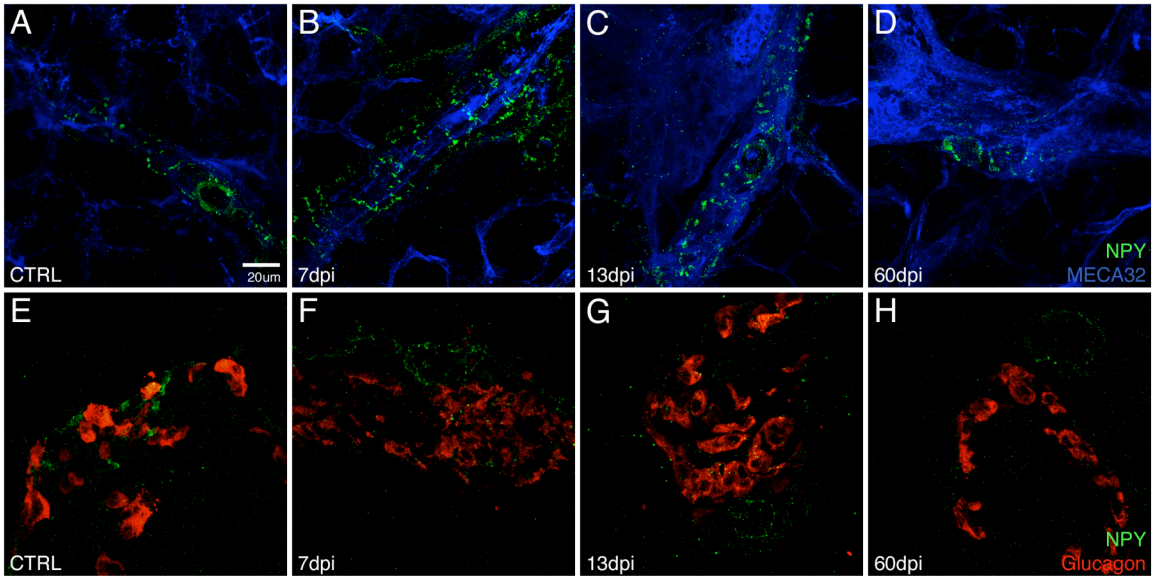


Figure 11: The structure of sympathetic fibers is intact throughout β-cell loss and resurgence. NPY-reactivity in sympathetic fibers (green, A-H) persists at perivascular plexuses along blood vessels (blue, A-D), and in close apposition to glucagon-producing α-cells (red, E-H). Control N=4; 7dpi N=4; 13dpi N=5; 60dpi N=5. Scale bar=20μm

Chapter 4: Discussion of Results and Their Implications

Innervation and encapsulation of islets occur in tandem with islet maturation

$VMAT2^+$ sympathetic and $CGRP^+$ sensory cell bodies migrate into the pancreatic bud from the neural tube, where they are detected at e10.5. Both are first detected in the pancreatic bud at e12.5. While CGRP is detected in sensory fibers soon after at e15.5, VMAT2 does not clearly mark sympathetic neural fibers until shortly after birth. Preliminary results indicate that NPY is present and marks sympathetic neural fibers as early as p0. Although embryonic analysis has not been conducted using NPY as a sympathetic marker, it is highly likely that NPY may be expressed in sympathetic fibers late in embryonic development, and possibly earlier. It remains to be shown whether outgrowth of NPY^+ sympathetic processes is temporally in line with the development of sensory processes.

The development of islet innervation by sympathetic and sensory neurons, and islet encapsulation by $GFAP^+$ astroglia, are closely integrated with postnatal islet maturation. All three of these neural crest derived populations are detected in close apposition to endocrine cells at or within a few days after birth. They then appear to coalesce with endocrine cells to form nascent islets during the first postnatal week, and adopt their adult position within islets by the second postnatal week. Meanwhile, the association of sympathetic tracts with blood vessels in the maturing postnatal pancreas is a unique developmental hallmark of postganglionic sympathetic neurons. At p7, the beginning of the second postnatal week, there is increasing complexity of early postnatal sympathetic association with the vasculature. By the beginning of the third postnatal week at p15, elaboration of the perivascular plexus closely resembles adult perivascular

morphology. In comparison, sensory perivascular association does not appear to become more elaborate during the course of pancreatic maturation.

The adult morphology of pancreatic innervation by the sympathetic and sensory nerve populations is similar in that observed neural fibers are enriched around the islet periphery compared to the islet core. By contrast, the nerve populations are distinct in their extents of islet innervation and in their modes of association with pancreatic blood vessels. Sympathetic islet innervation is greatly enriched in comparison to sensory islet innervation. $VMAT2^{+}$ (and NPY^{+}) sympathetic processes tend to fasciculate into tracts of multiple processes that surround pancreatic blood vessels in a perivascular plexus. $CGRP^{+}$ sensory processes are less fasciculated by comparison, and single processes tend to appear separate from particular blood vessels.

Many antigens that are ordinarily considered dependable neural markers are unfortunately unsuitable for use in the pancreas, either because fragile antigen markers have been destroyed by digestive enzymes, or because they are also displayed by various pancreatic endocrine cells, thus confounding a descriptive analysis. The neuronal and astroglial antibodies that we found suitable to our purpose had all been raised in rabbit hosts, and therefore could not be used simultaneously to compare the cell populations. However, the clear morphological differences among the three cell types studied, as well as previously published descriptions of adult staining patterns, convince us that antibodies raised against VMAT2, CGRP, and GFAP are respectively labeling sympathetic, sensory, and astroglial cells in our study.

The presence of VMAT2 provides clues to the status of autonomic function in developmental and disease states of the pancreas

Intracellular localization of VMAT2 to small synaptic vesicles (SSVs) and dense core vesicles (DCVs) has been reported in catecholaminergic neurons in the CNS (Nirenberg et al. 1995, 1996, 1997). Additionally, there is a wealth of evidence suggesting that peripheral sympathetic neurons modulate visceral responses through the slow, nonsynaptic release of monoamines from DCVs in axon terminals (Nirenberg et al. 1995; Vizi 1991; Beaudet and Descarries 1978). Monoamines can also be released from dendrites, occasionally by exocytosis from DCVs (Li et al. 2005; Nirenberg et al. 1995; Morris and Pow 1991; Geffen et al. 1976). The ultrastructural studies that would further define the intracellular localization of VMAT2 in postganglionic sympathetic pancreatic neurons have yet to be done. However, the subcellular $VMAT2^{+}$ localization in these neurons during postnatal maturation implies that postganglionic sympathetic neurons may be physiologically able to accumulate and secrete noradrenaline during maturation of the endocrine pancreas. Pancreatic neurons do not form true synapses with islet cells (Fisher and Bourque 2001; Fujita and Kobayashi 1979). While they contact target cells, to date there is no evidence to suggest the presence of postsynaptic densities that define the canonical synapse. Therefore, since early contacts between neurons and endocrine cells resemble the adult associations, it is possible that neuroendocrine signaling could be taking place before pancreatic islets are fully mature. Whether such signaling occurs, and concomitantly, whether that signaling has a role in directing the extent of pancreatic innervation during development, are open questions.

Sympathetic neurons, sensory neurons, and astroglia are differentially affected by large-scale fluctuations in the β–cell population

The RIP-cmyc^{ER} mouse line provides a disease model in which to explore the physiology of various adult pancreatic cell populations, both in response to a controlled large-scale depletion of β-cells and the resulting hyperglycemia that mimic type I diabetes, and during β-cell repopulation of the islets of Langerhans and recovery of normoglycemia. Observation of impaired glucose tolerance during high-stringency glucose tolerance tests after these animals were otherwise considered fully recovered (P. Heiser, personal communication) led us to hypothesize that autonomic islet innervation is affected, and that the recovery of some physiological aspect of autonomic innervation in these animals may not be complete after 60 days of recovery. Remodeling of pancreatic sensory neurons has been associated with pain in the context of pancreatic cancer (Lindsay et al. 2005). In contrast, pancreatic pain has not been reported in association with diabetic phenotypes. Hence the lack of detectable sensory remodeling in the RIP-cmyc^{ER} line is perhaps expected. Finally, changes in pancreatic astroglia have been previously reported in non-obese diabetic (NOD) mice, and we believed that our system would allow us to view astroglial remodeling in closer detail (Winer et al. 2003; Persson-Sjogren 2005).

As noted previously, the availability of antibodies suitable for pancreatic analysis necessarily limited our findings. Thus, the markers utilized in this study cannot provide an exhaustive description of sympathetic, sensory, and astroglial innervation. In addition, although the dimensional information contained in 50μm sections is far superior to that of thinner (5-10μm) sections, 50μm sections were not thick enough to provide a full 3-

dimensional rendering of labeled islets and neurons. Sections over 50μm thick yielded no more information, as 50μm was found to be the limit at which antibodies were fully able to penetrate sections. This technical limitation made it impossible to ascertain all the projections coming from a single neural or astroglial cell body, or to connect more distal projections with specific cell bodies. Similarly, in this study we were unable to ascertain whether projections from single neurons were sent to multiple islets, or to trace projections from specific intrapancreatic or extra-pancreatic ganglia to particular parts of the pancreas. Particularly in the context of β-cell regeneration, it is very possible that other changes that could be taking place in the neurons and astroglia but were missed in our analysis simply because we lacked markers adequate to observe and document them.

Response of sympathetic innervation to loss and replenishment of the β-cell population, and correlation of neural recovery with physiological recovery of the endocrine pancreas

Loss and recovery of VMAT2 reactivity in postganglionic sympathetic neurons temporally coincides with the incidence of hyperglycemia and the recovery of normoglycemia in RIP-cmyc^{ER} mice following tamoxifen insult. At 60dpi, we observe recovery of normal blood glucose levels coincident with the restoration of subcellular VMAT2 localization. The VMAT2 transporter molecule has a recognized role in the storage and transport of catecholamines, particularly in the modulation of monoamine neurotransmission in dopamine-producing cells in the central nervous system (CNS) (Nirenberg 1997). This transporter may have a similar function in peripheral sympathetic neurons. Since the pancreatic sympathetic neurons remain while VMAT2 immunoreactivity is lost, we conclude that the ability of postganglionic sympathetic

neurons to accumulate noradrenaline may be compromised by the large-scale loss of β-cells in RIP-cmyc^{ER} animals. However, the persistence of NPY localization indicates that the architecture of sympathetic neurons is maintained throughout changes in the β-cell population.

Loss of the β-cell population does not affect the subcellular localization of CGRP, a molecule that is central to nociception

Increased CGRP^{+} pancreatic sensory innervation has been implicated in pancreatic cancer-associated pain (Lindsay et al. 2005). Pancreatic pain has not been associated with β-cell loss itself-- as occurs in type 1 diabetes and in synthetic diabetic mouse models such as non-obese diabetic or streptozotocin mice. In the RIP-cmyc^{ER} model, CGRP-reactivity is retained in sensory fibers observed at islets. Additionally, no architectural changes are apparent during the loss and recovery of β-cells in RIP-cmyc^{ER} mice. These results underscore that the effects of β-cell loss on islet-associated neurons are specific to cell type, and not general effects of pancreatic ill health or islet deterioration.

Astroglial islet encapsulation is responsive to changes in islet state

Pancreatic astroglia appear to be affected by the large-scale loss and replenishment of beta cells, but the effect is distinct from observed effects on sympathetic fibers in that astroglial changes occur later in the blood glucose recovery curve than do changes in the sympathetic nerves. While the astroglial population diminishes in response

to β-cell loss, astroglial contact with islets as detected by GFAP reactivity is observed throughout the loss and replenishment of the β-cell population.

This transient decrease in islet encapsulation by astroglia appears to be a function of glial remodeling in response to changes in islet state; recovery of encapsulation also appears to be swift, indicating that there is a direct link between islet state and level of astroglial contact. This result is in keeping with the hypothesis that astroglia are performing a support role at the pancreatic islets.

It should be noted that islet encapsulation by astroglia appears to increase above wild type levels roughly 1-1.5 weeks after initiation of cmyc activation. We believe this is a visual artifact brought about by the loss of islet volume and surface area such that the ratio of astroglia to islet area has increased, rather than a true representation of astroglial increase. The exact function of pancreatic astroglia is unknown at this time. It is possible that there is a transient increase in encapsulation by astroglia as part of a response to physiological stress. This could then be followed by a transient astroglial decrease, either in response to a decrease in stress as recovery of the β-cell population begins, or in response to decreased islet size, and another increase in islet encapsulation as the islet is repopulated with β-cells and accordingly grows in size and nutritive need. A quantitative analysis of this phenomenon in three dimensions would be informative in this respect, as would genetic manipulation of possible molecules involved. The presence of the different protein markers assayed does provide some clues to the possibility of peripheral nervous system (PNS) function in both the developmental and islet recovery assays, but does not provide conclusive functional information about the cells visualized, nor can it conclusively link pancreatic neural function with pancreatic function. Further

morphological and functional analyses would have to be undertaken to conclusively define a role for PNS function during both pancreatic development and adult islet recovery.

There are a number of species-specific variations in the enteric nervous system (ENS), notably between large and small mammals (Faussone-Pellegrini 2006; Furness et al. 2006; reviewed in Hansen 2003a). These include differences in anatomical organization of the ENS as well as neurophysiology. Hence a direct analogy between these findings and the human context cannot automatically be assumed. Yet this study does contribute to a greater understanding of how physiological systems develop together and coordinate their functions, which can be highly instructive in terms of elucidating how permutation of one organ system through stress or disease can specifically affect parallel systems in an organism. Such an understanding may also have some interesting applications to islet transplantation biology. This analysis of endocrine innervation in the context of islet development and perturbation begins to clarify the relationship between endocrine pancreas development, physiology and innervation.

References

Adeghate, E., 2002. Pancreatic tissue grafts are reinnervated by neuro-peptidergic and cholinergic nerves within five days of transplantation. Transpl Immunol. 10, 73-80.

Adeghate, E., Ponery, A. S., Pallot, D. J. and Singh, J., 2000. Distribution of neurotransmitters and their effects on glucagon secretion from the in vitro normal and diabetic pancreatic tissues. Tissue Cell. 32, 266-274.

Ahren, B., 2006. The insulin response to gastric glucose is reduced in PAC1 and GRP receptor gene deleted mice. Nutr Met Cardiovasc Dis. 16, 517-521.

Ahren, B., 2000. Autonomic regulation of islet hormone secretion--implications for health and disease. Diabetologia. 43, 393-410.

Anlauf, M., Eissele, R., Schafer, M. K., Eiden, L. E., Arnold, R., Pauser, U., Kloppel, G. and Weihe, E., 2003. Expression of the two isoforms of the vesicular monoamine transporter (VMAT1 and VMAT2) in the endocrine pancreas and pancreatic endocrine tumors. J Histochem Cytochem. 51, 1027-1040.

Beaudet, A. and Descarries, L., 1978. The monoamine innervation of rat cerebral cortex: synaptic and nonsynaptic axon terminals. Neuroscience. 3, 851-860.

Benthem, L., Mundinger, T. O. and Taborsky, G. J., Jr., 2001. Parasympathetic inhibition of sympathetic neural activity to the pancreas. Am J Physiol Endocrinol Metab. 280, E378-381.

Berggren, P. O. and Leibiger, I. B., 2006. Novel aspects on signal-transduction in the pancreatic beta-cell. Nutr Metab Cardiovasc Dis. 16 Suppl 1, S7-10.

Bronner-Fraser, M., 1993. Neural crest cell migration in the developing embryo. Trends Cell Biol. 11, 392-397.

Durant, S., Geutskens, S., Van Blokland, S. C., Coulaud, J., Alves, V., Pleau, J. M., Versnel, M., Drexhage, H. A. and Homo-Delarche, F., 2003. Proapoptosis and antiapoptosis-related molecules during postnatal pancreas development in control and nonobese diabetic mice: relationship with innervation. Lab Invest. 83, 227-239.

Edwards, R. H., Rutter, W. J. and Hanahan, D., 1989. Directed expression of NGF to pancreatic beta cells in transgenic mice leads to selective hyperinnervation of the islets. Cell. 58, 161-170.

Faussone-Pellegrini, M. S., 2006. Relationships between neurokinin receptor-expressing interstitial cells of Cajal and tachykininergic nerves in the gut. J Cell Mol Med. Jan-Mar, 1, 20-32.

Fisher, T. E. and Bourque, C. W., 2001. The function of Ca(2+) channel subtypes in exocytotic secretion: new perspectives from synaptic and non-synaptic release. Prog Biophys Mol Biol. 77, 269-303.

Franke, D. D. H., Yolcu, E. S., Alard, P., Kosciewicz, M. M., Shirwan, H., 2007. A novel multimeric form of FasL modulates the ability of diabetogenic T cells to mediate type 1 diabetes in an adoptive transfer model. Molec Immunol. 11, 2884-2892.

Fujita, T. and Kobayashi, S., 1979. Proposal of a neurosecretory system in the pancreas. An electron microscope study in the dog. Arch Histol Jpn. 42, 277-295.

Furness, J. B., Hind, A. J., Ngui, K., Robbins, H. L., Clerc, N., Merrot, T., Tjandara, J. J., Poole, D. P., 2006. The distribution of PKC isoforms in enteric neurons, muscle, and interstitial cells of the human intestine. Histochem Cell Biol. 5, 537-548.

Geffen, L. B., Jessell, T. M., Cuello, A. C. and Iversen, L. L., 1976. Release of dopamine from dendrites in rat substantia nigra. Nature. 260, 258-260.

Graham, A., 2003. The Neural Crest. Curr Biol. 10, R381-R384.

Grodsky, G. M., Ma, Y. H. and Edwards, R. H., 1997. Chronic sympathetic innervation of islets in transgenic mice results in differential desensitization of alpha-adrenergic inhibition of insulin secretion. Adv Exp Med Biol. 426, 129-138.

Halassa, M. M., Fellin, T. and Haydon, P. G., 2007. The tripartite synapse: roles for gliotransmission in health and disease. Trends Mol Med. 13, 54-63.

Hansen, M. B., 2003. The enteric nervous system I: organisation and classification. Pharmacol Toxicol. 92, 105-113.

Hansen, M. B., 2003. The enteric nervous system II: gastrointestinal functions. Pharmacol Toxicol. 92, 249-257.

Hari, L., Brault, V., Kleber, M., Lee, H.-Y., Ille, F., Leimeroth, R., Paratore, C., Suter, U., Kemler, R. and Sommer, L., 2002. Lineage-specific requirements of beta-catenin in neural crest development. Journal of Cell Biology. 159, 867-880.

Homo-Delarche, F., 2004. Neuroendocrine immuno-ontogeny of the pathogenesis of autoimmune disease in the nonobese diabetic (NOD) mouse. Ilar J. 45, 237-258.

Kasemeier-Kulesa, J. C., Kulesa, P. M. and Lefcort, F., 2005. Imaging neural crest cell dynamics during formation of dorsal root ganglia and sympathetic ganglia. Development. 132, 235-245.

Kawahira, H., Scheel, D. W., Smith S. B., German M. S., Hebrok, M., 2005. Hedgehog signaling regulates expansion of pancreatic epithelial cells. Dev Biol. 280(1), 111-121.

Kawahira, H., Ma, M. H., Tzanakakis, E. S., McMahon, A. P., Chuang, P. T., Hebrok, M, 2003. Combined activities of hedgehog signaling inhibitors regulate pancreas development. Development. 130(20), 4871-4879.

Kessler, J. A., 1985. Parasympathetic, sympathetic, and sensory interactions in the iris: nerve growth factor regulates cholinergic ciliary ganglion innervation in vivo. J Neurosci. 5, 2719-2725.

Kiba, T., 2004. Relationships between the autonomic nervous system and the pancreas including regulation of regeneration and apoptosis: recent developments. Pancreas. 29, e51-58.

Kim, S. K. and Hebrok, M., 2001. Intercellular signals regulating pancreas development and function. Genes Dev. 15, 111-127.

Konturek, S. J., Zabielski, R., Konturek, J. W. and Czarnecki, J., 2003. Neuroendocrinology of the pancreas; role of brain-gut axis in pancreatic secretion. Eur J Pharmacol. 481, 1-14.

Li, H., Waites, C. L., Staal, R. G., Dobryy, Y., Park, J., Sulzer, D. L. and Edwards, R. H., 2005. Sorting of vesicular monoamine transporter 2 to the regulated secretory pathway confers the somatodendritic exocytosis of monoamines. Neuron. 48, 619-633.

Lindsay, T. H., Halvorson, K. G., Peters, C. M., Ghilardi, J. R., Kuskowski, M. A., Wong, G. Y. and Mantyh, P. W., 2006. A quantitative analysis of the sensory and sympathetic innervation of the mouse pancreas. Neuroscience. 137, 1417-1426.

Lindsay, T. H., Jonas, B. M., Sevcik, M. A., Kubota, K., Halvorson, K. G., Ghilardi, J. R., Kuskowski, M. A., Stelow, E. B., Mukherjee, P., Gendler, S. J., Wong, G. Y. and Mantyh, P. W., 2005. Pancreatic cancer pain and its correlation with changes in tumor vasculature, macrophage infiltration, neuronal innervation, body weight and disease progression. Pain. 119, 233-246.

Mei, Q., Mundinger, T. O., Lernmark, A. and Taborsky, G. J., Jr., 2002. Early, selective, and marked loss of sympathetic nerves from the islets of BioBreeder diabetic rats. Diabetes. 51, 2997-3002.

Morris, J. F. and Pow, D. V., 1991. Widespread release of peptides in the central nervous system: quantitation of tannic acid-captured exocytoses. Anat Rec. 231, 437-445.

Mundinger, T. O., Mei, Q., Figlewicz, D. P., Lernmark, A. and Taborsky, G. J., Jr., 2003. Impaired glucagon response to sympathetic nerve stimulation in the BB diabetic rat: effect of early sympathetic islet neuropathy. Am J Physiol Endocrinol Metab. 285, E1047-1054.

Nathan, J. D., Peng, R. Y., Wang, Y., McVey, D. C., Vigna, S. R. and Liddle, R. A., 2002. Primary sensory neurons: a common final pathway for inflammation in experimental pancreatitis in rats. Am J Physiol Gastrointest Liver Physiol. 283, G938-946.

Newgreen, D. and Young, H. M., 2002. Enteric nervous system: development and developmental disturbances--part 1. Pediatr Dev Pathol. 5, 224-247.

Newgreen, D. and Young, H. M., 2002. Enteric nervous system: development and developmental disturbances--part 2. Pediatr Dev Pathol. 5, 329-349.

Nirenberg, M. J., Chan, J., Liu, Y., Edwards, R. H. and Pickel, V. M., 1996. Ultrastructural localization of the vesicular monoamine transporter-2 in midbrain dopaminergic neurons: potential sites for somatodendritic storage and release of dopamine. J Neurosci. 16, 4135-4145.

Nirenberg, M. J., Chan, J., Liu, Y., Edwards, R. H. and Pickel, V. M., 1997. Vesicular monoamine transporter-2: immunogold localization in striatal axons and terminals. Synapse. 26, 194-198.

Nirenberg, M. J., Chan, J., Vaughan, R. A., Uhl, G. R., Kuhar, M. J. and Pickel, V. M., 1997. Immunogold localization of the dopamine transporter: an ultrastructural study of the rat ventral tegmental area. J Neurosci. 17, 5255-5262.

Nirenberg, M. J., Liu, Y., Peter, D., Edwards, R. H. and Pickel, V. M., 1995. The vesicular monoamine transporter 2 is present in small synaptic vesicles and preferentially localizes to large dense core vesicles in rat solitary tract nuclei. Proc Natl Acad Sci U S A. 92, 8773-8777.

Pelengaris, S., Khan, M. and Evan, G. I., 2002. Suppression of Myc-induced apoptosis in beta cells exposes multiple oncogenic properties of Myc and triggers carcinogenic progression. Cell. 109, 321-334.

Persson-Sjogren, S., 2001. Neuroinsular complex type I: morphology and frequency in lean and genetically obese mice. Pancreas. 23, 40-48.

Persson-Sjogren, S., Forsgren, S., Shi, C. L. and Taljedal, I. B., 2001. Mouse islets cultured with vasoactive intestinal polypeptide: effects on insulin release and immunoreactivity for tyrosine hydroxylase. Pancreas. 22, 84-90.

Persson-Sjogren, S., Forsgren, S. and Taljedal, I. B., 1998. Expression of tyrosine hydroxylase, calcitonin gene-related peptide, substance P and protein gene product 9.5 in mouse islets transplanted under the kidney capsule. Neuropeptides. 32, 307-318.

Persson-Sjogren, S., Forsgren, S. and Taljedal, I. B., 2000. Peptides and other neuronal markers in transplanted pancreatic islets. Peptides. 21, 741-752.

Persson-Sjogren, S., Holmberg, D. and Forsgren, S., 2005. Remodeling of the innervation of pancreatic islets accompanies insulitis preceding onset of diabetes in the NOD mouse. J Neuroimmunol. 158, 128-137.

Persson-Sjogren, S., Zashihin, A. and Forsgren, S., 2001. Nerve cells associated with the endocrine pancreas in young mice: an ultrastructural analysis of the neuroinsular complex type I. Histochem J. 33, 373-378.

Rossi J., Santamaki P., Airaksinen M. S., Herzig K.H, 2005. Parasympathetic innervation and function of endocrine pancreas requires the glial cell line-derived factor family receptor alpha2 (GFRalpha2). Diabetes. 5, 1324-1330.

Saravia, F. and Homo-Delarche, F., 2003. Is innervation an early target in autoimmune diabetes? Trends Immunol. 24, 574-579.

Serizawa, Y., Kobayashi, S. and Fujita, T., 1979. Neuro-insular complex type I in the mouse. Re-evaluation of the pancreatic islet as a modified ganglion. Arch Histol Jpn. 42, 389-394.

Sudhof, T. C., 1995. The synaptic vesicle cycle: a cascade of protein-protein interactions. Nature. 375, 645-653.

Vizi, E. S., 1991. Evidence that catecholamines increase acetylcholine release from neuromuscular junction through stimulation of alpha-1 adrenoceptors. Naunyn Schmiedebergs Arch Pharmacol. 343, 435-438.

Weihe, E. and Eiden, L. E., 2000. Chemical neuroanatomy of the vesicular amine transporters. Faseb J. 14, 2435-2449.

Wick, E. C., Hoge, S. G., Grahn, S. W., Kim, E., Divino, L. A., Grady, E. F., Bunnett, N. W. and Kirkwood, K. S., 2006. Transient receptor potential vanilloid 1, calcitonin gene-related peptide, and substance P mediate nociception in acute pancreatitis. Am J Physiol Gastrointest Liver Physiol. 290, G959-969.

Wick, E. C., Pikios, S., Grady, E. F. and Kirkwood, K. S., 2006. Calcitonin gene-related peptide partially mediates nociception in acute experimental pancreatitis. Surgery. 139, 197-201.

Winer, S., Tsui, H., Lau, A., Song, A., Li, X., Cheung, R. K., Sampson, A., Afifiyan, F., Elford, A., Jackowski, G., Becker, D. J., Santamaria, P., Ohashi, P. and Dosch, H. M., 2003. Autoimmune islet destruction in spontaneous type 1 diabetes is not beta-cell exclusive. Nat Med. 9, 198-205.

Yi S.Q., Miwa K., Ohta T., Kayahara M., Kitagawa H., Tanaka A., Shimokawa T., Akita K., Tanaka S., 2003. Innervation of the pancreas from the perspective of perineural invasion of pancreatic cancer. Pancreas. 3, 225-229.

Yokoyama-Hayashi, K., Takahashi, T., Kakita, A. and Yamashina, S., 2002. Expression of PGP9.5 in ductal cells of the rat pancreas during development and regeneration: can it be a marker for pancreatic progenitor cells? Endocr J. 49, 61-74.

Table 1: Antibodies Used in Published Analysis

Antibody	Source	Conditions
Rabbit anti rat VMAT2	Phoenix	1:400 16 hours 4°C
Rabbit anti CGRP	Sigma	1:700 16 hours 4°C
Rabbit anti GFAP	Signet	1:50 16 hours 4°C
Rabbit anti Neuropeptide Y	Chemicon	1:400 16 hours 4°C
Guinea pig anti Insulin	Linco	1:400 16 hours 4°C
Guinea pig anti Glucagon	Linco	1:400 16 hours 4°C
Guinea pig anti Pancreatic Polypeptide	Linco	1:1000 16 hours 4°C
Rat anti Somatostatin	Chemicon	1:200 16 hours 4°C
Rat anti MECA32	BD Pharmingen	1:200 16 hours 4°C
Donkey anti Rabbit Alexa Fluor 488	Molecular Probes	1:500 16 hours 4°C
Goat anti Guinea pig Alexa Fluor 633	Molecular Probes	1:500 16 hours 4°C
Goat anti Rat Cy3	Jackson	1:200 16 hours 4°C

Table 2: **Additional Antibodies Assayed (not used in published analysis)**

Antibody	Source	Conditions Tried*
Chicken anti MAP2	Abcam	1:200-1:1000
Chicken anti VAMP2	Abcam	1:200-1:1000
Guinea pig anti Substance P	Chemicon	1:200
Mouse monoclonal anti Tu20 (tubulin)	Chemicon	1:50-1:100
Mouse monoclonal anti Discs Large (DLG)	Graeme Davis' Lab	1:500
Mouse monoclonal anti Glutamate Receptor II A	Graeme Davis' Lab	1:10
Mouse monoclonal anti NC82	Graeme Davis' Lab	1:20
Mouse monoclonal anti Synapsin	Graeme Davis' Lab	1:8
Mouse monoclonal anti SAP47	Graeme Davis' Lab	1:30-1:60
Rabbit anti Tyrosine Hydroxylase	Chemicon	1:200
Rabbit anti GRP	Research Diagnostics, Inc.	1:10
Rabbit anti GRP	Maine Biotech	1:400-1:800
Rabbit anti Ghrelin	Phenix	1:200
Rabbit anti PACAP38	Phoenix	1:200
Goat anti chicken Cy5	Abcam	1:200
Avidin DCS anti mouse Cy3	Jackson	1:200-1:300
Goat anti Mouse Alexa Fluor 488	Molecular Probes	1:500
Goat anti Rabbit Alexa Fluor 647	Molecular Probes	1:500

*All trials conducted overnight at 4°C.

Appendix 1: Representative Controls

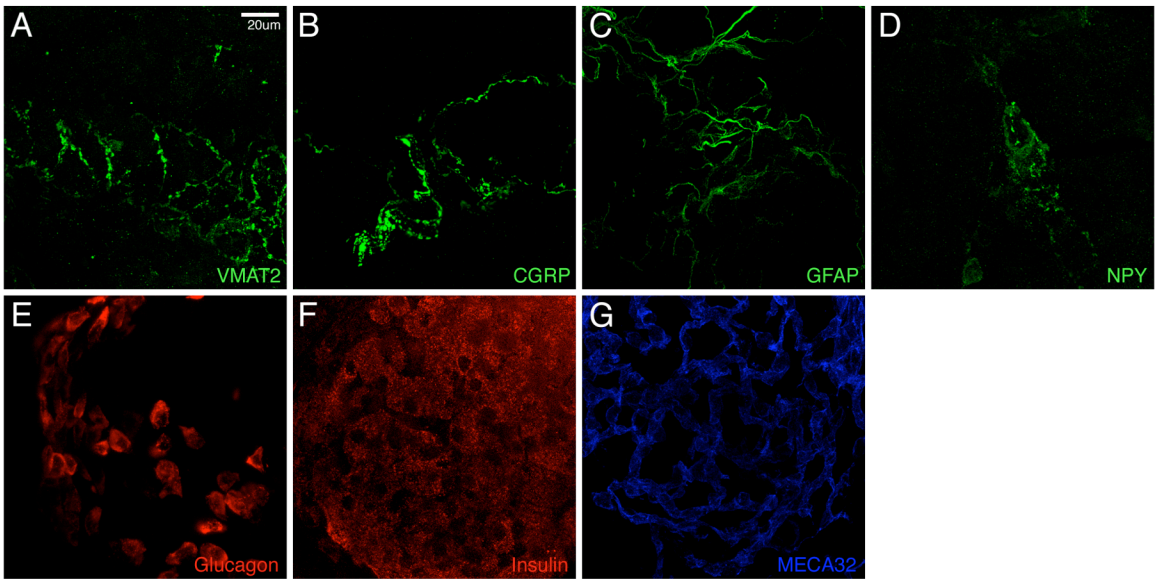


Figure 12: Positive control stainings for the antibodies featured in this analysis. The above are wild-type tissues, each treated with a single primary antibody as labeled (see Table 1 for antibody information). The antibodies lacked significant overlap. These are representative of positive control results obtained throughout the study. Scale bar=20μm

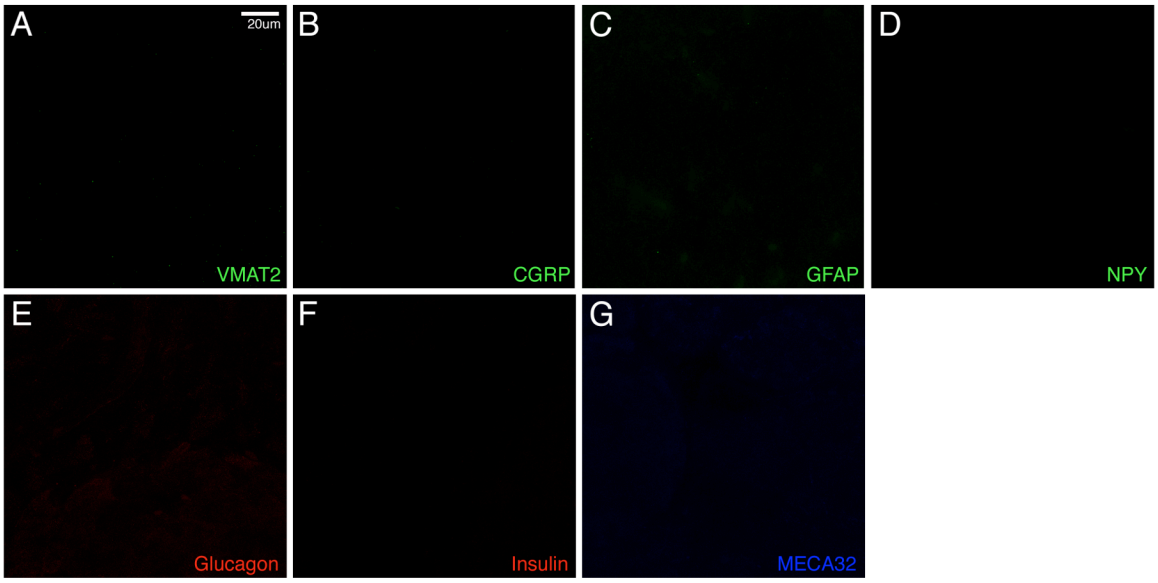


Figure 13: Negative control stainings for the antibodies featured in this analysis. The above are wild-type adult tissues, each untreated with a single primary antibody as labeled (see Table 1 for antibody information). The antibodies were found to have low relative background. These are representative of negative control results obtained throughout the study. Scale bar=20μm

Appendix 2: Unpublished Results and Their Implications

In addition to the confocal analysis that has been published, attempts were made to complete a comparable analysis of GRP^{+} parasympathetic neurons in wild type CD1 and RIP-$cmyc^{ER}$ transgenic animals, as well as to ascertain whether perturbations in the developmental timetable of the endocrine pancreas had any affects on pancreatic neural development, and whether neuroendocrine remodeling in non-obese diabetic (NOD) mice was limited to particular neural subtypes. These additional efforts were met with varying degrees of success, as is described below.

Sympathetic nerve development appears unperturbed in Pax4-Shh transgenic mice

Pax4-Shh mice express the Sonic hedgehog protein under the control of the human Pax4 promoter, which induces Hedgehog expression midway through pancreas development. At E18.5, the time point when endocrine cells first cluster in wild type embryos, islet morphology is severely impaired in Pax4-Shh mice. Pax4-Shh transgenic mice have a transient phenotype in which the maturation of pancreatic islets is retarded during the first postnatal week. Endocrine cells still cluster eventually; however, the average size of the islets is significantly reduced and approximately 80% of the overall endocrine area is lost in transgenic mice. This is a transient phenotype; rigorous observation has revealed no morphological or physiological difference between transgenic mice and wild type littermates after p14 (Kawahira et al. 2005).

Immunofluorescent analysis of Pax4-Shh transgenic pups and their wild type C57BL/6 littermates from p0-p15 indicated that outgrowth of sympathetic fibers is not directly coupled to islet maturation. If the two were directly coupled, then the slowing of

islet maturation and endocrine migration/shuffling should result in either a concomitant transient slowing of fiber elongation or misdirection of sympathetic fibers, and might even have a permanent affect on sympathetic islet innervation. On the contrary, sympathetic fibers in Pax4-Shh transgenic mice were found to elongate and to become closely positioned next to alpha cells in a manner similar to that found in wild type littermates, and irrespective of whether those alpha cells appeared to be associated with a maturing islet. Furthermore, islet innervation in adolescent transgenic pups was not discernibly different from that of wild type littermates. It appears that sympathetic fibers are capable of forming the necessary close contacts with α-cells regardless of whether pancreatic islets are being formed on schedule.

The lack of any easily observable sympathetic neuronal phenotype in Pax4-Shh transgenic animals dictated that further study of them not be pursued in this analysis. It should be noted, however, that no quantitative analyses, such as counting of neuro-endocrine associations or measurement of sympathetic fiber elongation were undertaken; it is therefore possible that a subtler phenotype may exists.

Partial analysis of parasympathetic pancreatic neurons

An antibody raised against bombesin/ gastrin-releasing protein (GRP) was used to visualize postganglionic sympathetic and parasympathetic neuronal processes in the mouse pancreas. GRP^+ staining was observed only in GRP^+ neurons. As in the case of $VMAT2^+$and $CGRP^+$ fibers, GRP^+ fibers enter pancreatic islets at multiple points, and appear to be concentrated/enriched at the islet periphery (13A, B). Parasympathetic (GRP^+) neuronal processes appear to resemble sensory fibers both in the extent of islet

association and in their pattern of perivascular association in the adult mouse (Figure 13C).

GRP is not a marker of parasympathetic nerve growth and islet innervation during embryogenesis (e9.5-e18.5)

Although an antibody raised against GRP has proved to be highly useful in the detection of parasympathetic neurons at adult stages, it has unfortunately not been as informative during pancreas organogenesis and maturation. This is perhaps unsurprising, as the gastrin releasing protein molecule is involved in feeding and satiety cues that are not in play at embryonic stages, and highly changeable feeding behavior before weaning may have confounded assessments of GRP in neonates. At this time we have not identified a suitable marker to aid in the description of parasympathetic neural development in the pancreas.

Loss of β-cells in RIP-cmyc^{ER} mice appears to have an intermediate effect on parasympathetic islet innervation

Loss of beta cells has a heterogeneous and permanent effect on parasympathetic innervation

The observed interruption of parasympathetic islet innervation, as with the interruption of sympathetic islet innervation, occured during the initial loss of β-cells, as GRP reactivity was also lost by 7dpi. However, the observed loss of GRP reactivity in neural fibers was heterogeneous within the pancreas: GRP reactivity was lost from endocrine-associated parasympathetic fibers, but was retained in many perivascular

parasympathetic fibers not visibly associated with islets (Figure 14A, B). Tissues at 9dpi closely resembled those examined at 7dpi, but slight GRP activity was occasionally observed at islets that were associated with large blood vessels (Figure 14C). GRP reactivity was detected in perivascular fibers throughout the process of cmyc-triggered β-cell loss and islet repopulation (Figure 14D). The abrogation of GRP reactivity in islet-associated parasympathetic fibers does not appear to be amenable to recovery; GRP reactivity had not reappeared in islet-associated fibers by 60dpi, although normoglycemia had been attained as measured by random blood glucose tests (Figure 14E).

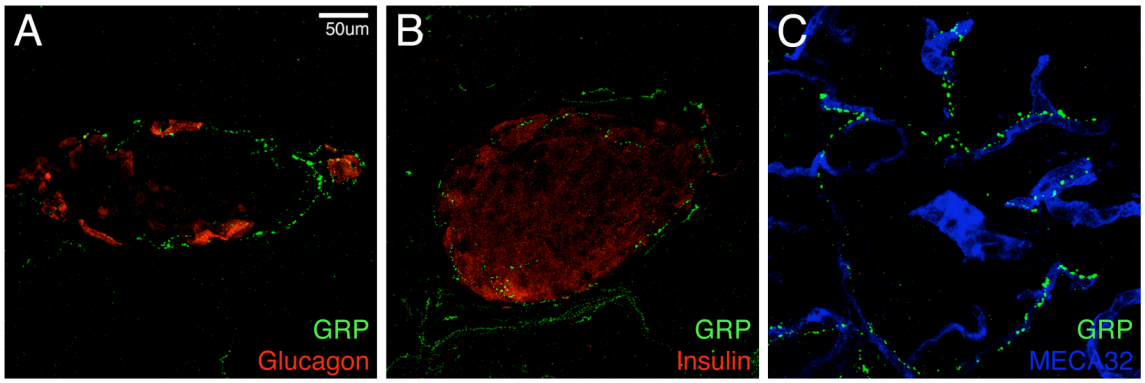


Figure 14: Pancreatic parasympathetic innervation has similarities with that of other neuronal subtypes. As in the case of sympathetic and sensory neurons, parasympathetic neural fibers in the adult mouse pancreas appear concentrated at the islet periphery defined by glucagon-producing α-cells (red, A), relative to the islet core defined by insulin-producing β-cells (red, B). Perivascular association resembles that of sensory fibers regarding their degree of fasciculation and alignment with blood vessels. N=8. Scale bar=50μm

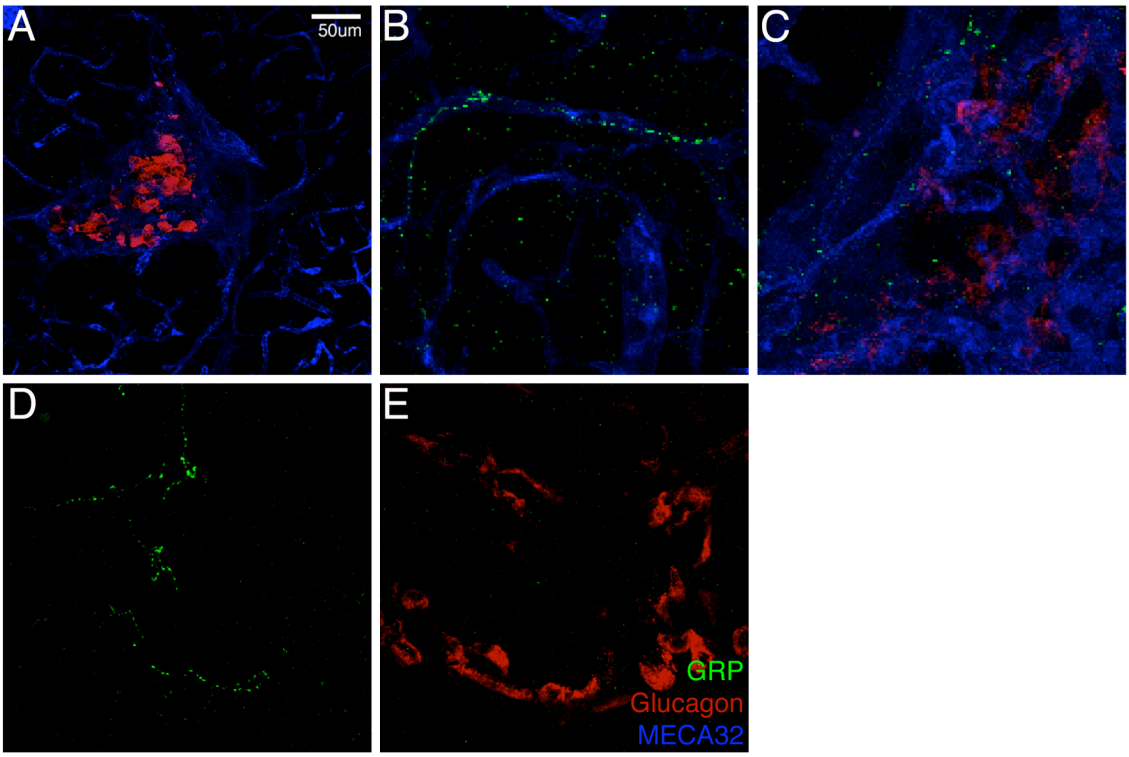


Figure 15: Loss of β-cells in RIP-cmyc^{ER} mice appears to have an intermediate effect on parasympathetic islet innervation. At 7dpi, GRP-reactivity is lost from islet-associated parasympathetic fibers (A), but retained in perivascular fibers that are not islet-associated (B). Tissues at 9dpi closely resembled those examined at 7dpi, but slight GRP activity was occasionally observed at islets that were associated with large blood vessels (C). Perivascular GRP persisted at 13dpi (D), while GRP reactivity remained absent from islets at 60dpi (E). N=2. Scale bar=50μm

In tamoxifen-injected RIP-cmyc^{ER} animals, GRP localization appeared to be simultaneously retained in many perivascular parasympathetic fibers and completely abolished in islet-associated parasympathetic fibers. This loss of islet-associated parasympathetic GRP localization was not recovered in the time that it takes RIP-cmyc^{ER} animals to regain normoglycemia following tamoxifen injection. Thus, loss of β-cells appears to affect the physiology of islet-associated parasympathetic fibers without affecting perivascular parasympathetic innervation. Furthermore, it appears that the GRP-secretory function of parasympathetic islet innervation is not strictly required for the recovery of normoglycemia in this context. Interestingly, the ability of RIP-cmyc^{ER} animals to process glucose is not completely normal after 60 days; it has been observed that although RIP-cmyc^{ER} mice are comparable to wild type littermates in terms of both their randomly tested blood glucose levels, and their ability to respond to standard glucose tolerance tests, their ability to respond to high-stringency glucose tolerance tests is limited compared to that of wild type animals (D. Cano and P. Heiser, unpublished observations). It has been shown previously that activation of the GRP receptor in β-cells accounts for a small percentage of glucose tolerance in response to gastrically (as opposed to intravenously) administrated glucose (Ahren 2006); one possibility is that the controlled release of GRP directly at islets may act in the fine-tuning of blood glucose level, without being strictly necessary for the systematic modulation of insulin release in response to high blood glucose. It remains to be determined when, if ever, RIP-cmyc^{ER} mice fully recover wild-type glucose tolerance in high-stringency tests, and whether this recovery coincides with the reconstitution of GRP localization in islet-innervating parasympathetic neurons. It should also be noted that the unsuitability of anti-GRP

antibodies for developmental analysis made it difficult to have full confidence in these results. Confirmation of these results with another marker specific to parasympathetic neurons is definitely desirable, but it was not possible to find a more suitable marker while this analysis was being carried out.

A preliminary comparative analysis of autonomic innervation in the non-obese diabetic (NOD) mouse

The non-obese diabetic (NOD) mouse line was isolated as a spontaneously occurring mutation in which the onset of a diabetic phenotype bears close resemblance to type 1 diabetes in humans. Islets in the NOD mouse are known to come under auto-immunologic attack by CD4 and CD8 T-cells, resulting in the loss of pancreatic β-cells and the onset of a diabetic phenotype at roughly 30 weeks of age. Onset of diabetes is preceded by islet inflammation, or "insulitis", and followed by measurable neuropathy in the long term, similar to human type 1 diabetes. By 1 year of age, sciatic neuropathy is clearly observable in NOD mice.

Remodeling of neural projections at pancreatic islets has been observed in conjunction with the autoimmune response and resulting insulitis that precede diabetes in NOD mice (Homo-Delarche 2004; Persson-Sjogren et al. 2005). This is likely to be analogous to the neuro-endocrine situation in humans, as it is known that multiple cell types are affected in autoimmune diabetes in humans (Winer et al. 2003). However, Persson-Sjogren's analysis relied on pan-neuronal and astroglial markers (PGP9.5 and GFAP, respectively), thus it remained unclear whether the observed neuro-endocrine remodeling involved particular neuron subtypes or was pan-neuronal in its effects.

NOD mice aged 18 weeks were subjected to confocal immunofluorescent analysis, and both VMAT2 and GRP reactivity were affected. These results closely resemble those found in the RIP-cmyc^{ER} mice shortly after tamoxifen-induced loss of β-cells. In particular, VMAT2-reactivity was abrogated from both peri-islet and perivascular sympathetic fibers, while GRP-reactivity was interrupted in peri-islet parasympathetic fibers, but persisted in perivascular fibers (Figure 15A-C). Analysis of astroglia using the GFAP marker was also performed as a positive control, and results of this analysis support Persson-Sjogren's findings. Thus, neuro-endocrine remodeling of both sympathetic and parasympathetic fibers appears to take place, in addition to the previously observed astroglial remodeling.

The exact relationship between the islet inflammation reported in NOD mice and the loss of sympathetic and parasympathetic pancreatic innervation markers is unknown. Rag1^{null} knockout mice are unable to mount an inflammatory response. NOD/Rag1^{null} double knockout mice lack functional T and B cells and do not spontaneously develop diabetes because they are deficient in RAG1, the gene responsible for V(D)J recombination in immunoglobulin and T-cell receptor genes (Franke et al. 2007). Hence, islet inflammation is suppressed in NOD/RAG double knockouts. We therefore elected to subject NOD/RAG double knockout mice to confocal analysis, to determine whether sympathetic and parasympathetic innervation were affected in the absence of an inflammatory response. Preliminary results indicate that VMAT2 and GRP are both present in the islet-associated neural fibers of NOD/RAG mice aged 18 weeks (Figure 15D and E).

Since β-cell loss in RIP-cmyc^{ER} and NOD models arises from variant circumstances (only the NOD model is directly based in the autoimmune response), their effects on neuronal subpopulations may differ. It would be interesting to determine whether neuro-endocrine remodeling in NOD mice affects sensory neurons that innervate islets as well. Analysis of sensory CGRP^{+} neurons was not undertaken in NOD mice due to time constraints, and therefore it remains unknown whether the neuro-endocrine remodeling that takes place in NOD mice, compared with the described results regarding the RIP-cmyc^{ER} regeneration model. Additionally, the described results have only been compiled for three mice, and have not been quantitated by further methods. Thus, they must be considered strictly preliminary.

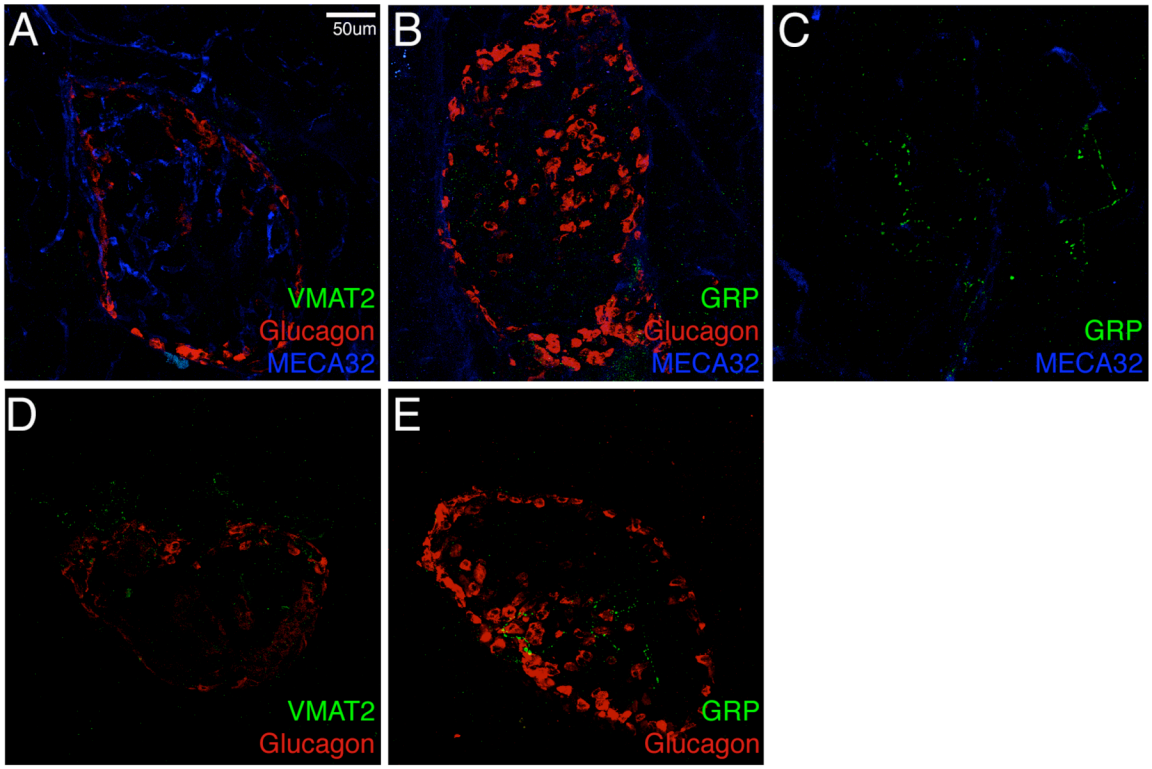


Figure 16: Sympathetic and parasympathetic neurons appear to be affected in NOD mice at 18 weeks of age. VMAT2-reactivity and GRP-reactivity appear to be greatly diminished in the islet-associated fibers of NOD mice (A and B), while GRP-reactivity persists in non-islet-associated perivascular parasympathetic fibers (C). However, $VMAT2^{+}$ and GRP^{+} fibers are clearly visible in islet-associated fibers of NOD/RAG double knock-out mice of the same age (D and E). N=3. Scale bar=50μm

Publishing Agreement

It is the policy of the University to encourage the distribution of all theses and dissertations. Copies of all UCSF theses and dissertations will be routed to the library via the Graduate Division. The library will make all theses and dissertations accessible to the public and will preserve these to the best of their abilities, in perpetuity.

Please sign the following statement:

I hereby grant permission to the Graduate Division of the University of California, San Francisco to release copies of my thesis or dissertation to the campus library to provide access and preservation, in whole or in part, in perpetuity.

Regina Burns
Author Signature

30 August 2007
Date